Partial-Duplex Amplify-and-Forward Relaying: Spectral Efficiency Analysis under Self-Interference

Roberto López-Valcarce, *Member, IEEE*, Carlos Mosquera, *Senior Member, IEEE*

***Abstract*—We propose a novel mode of operation for Amplify-and-Forward relays in which the spectra of the relay input and output signals partially overlap. This *partial-duplex* relaying mode encompasses half- and full-duplex as particular cases. By viewing the partial-duplex relay as a bandwidth-preserving Linear Periodically Time-Varying system, a spectral efficiency analysis under self-interference is developed. In contrast with previous works, self-interference is regarded as a useful information-bearing component rather than simply assimilated to noise. This approach reveals that previous results regarding the impact of self-interference on (full-duplex) relay performance are overly pessimistic. Based on a frequency-domain interpretation of the effect of self-interference, a number of suboptimal decoding architectures at the destination node are also discussed. It is found that the partial-duplex relaying mode may provide an attractive tradeoff between spectral efficiency and receiver complexity.**

I. Introduction

Relay-assisted communication is a widespread technique to extend coverage and improve reliability of wireless networks [2], [3]. Depending on how the received signal is processed by the relay node, a number of relaying schemes can be identified. Among these, Amplify-and-Forward (A&F), in which the relay just amplifies the received signal and then forwards it to the destination, emerges as a highly flexible technology, which is transparent to the particular modulation type of the retransmitted signal and has low implementation complexity [4], [5]. Traditionally, A&F relays operate in Half-Duplex (HD) mode: they transmit and receive either at different times, or over sufficiently separated frequency bands. This is because simultaneously transmitting and receiving on the same band would result in strong self-interference (SI) many tens of dB above the signal of interest, potentially overwhelming the receiver. This Full-Duplex (FD) mode, however, is of great interest for next-generation wireless systems due to its potential to improve spectral efficiency by avoiding the use of additional time or frequency resources [6]–[9]. This has motivated the study of SI cancellation technologies [10]–[13], with results suggesting that operation in FD mode may be feasible. In fact, FD A&F relaying is already found in certain practical settings such as on-frequency repeaters for broadcasting applications [14]–[16]. Nevertheless, given the high SI levels present in practice, some residual SI is to be expected in most scenarios, as perfect cancellation is generally not possible [8], [9]. Thus, analyzing the impact of SI in the performance of FD transceivers in general, and in FD A&F relay networks in particular, has significant interest.

A number of such analyses, under different assumptions, can be found in the literature. In many of these, the residual SI is modeled as (usually Gaussian) noise, statistically independent of the signal of interest, and whose power depends in some way on the power of the signal transmitted by the relay [17]–[21]. The Gaussian assumption is usually justified by invoking the Central Limit Theorem, given the variety of sources of imperfection in the cancellation process; whereas the independence assumption may be motivated by assuming a sufficiently large processing delay effectively decorrelating the relay transmit signal with the simultaneously received signal [22]. In fact, this relay processing delay lies at the core of the problem, because when the processing delay is negligible (i.e., the delay-bandwidth product is much smaller than one), SI ceases to be harmful as its effect can be assimilated to a mere scaling [23], [24].

All the aforementioned works hinge on the assumption that SI can be regarded as noise. This is rather pessimistic, because the SI waveform contains useful information about the signal transmitted by the source. To the best of our knowledge, the only related works in which the receiver at the destination exploits SI in the decoding process are [25] and [26], which assume that there is exactly a one-symbol delay for the relay to forward its received symbols. We build upon this possibility and investigate the impact on spectral efficiency for an FD A&F relay without placing constraints on its processing delay. Our analysis shows that such approach results in a much more graceful performance degradation compared to the standard procedure of treating SI as noise.

Specifically, we study the performance of a single-input single-output (SISO) A&F relay with automatic gain control under a novel *Partial Duplexing* (PD) operation mode, in which the relay transmits and receives simultaneously, placing the transmitted signal in a frequency band that *partially* overlaps with that of the incoming signal. Thus, HD and FD are obtained as particular instances of PD with zero and 100% overlap, respectively. It must be noted that PD is fundamentally different from previous hybrid approaches [22], [27], which opportunistically switch between HD and FD modes depending on link quality; in contrast, channel state information is not needed at the relay in PD mode, so that relay operation remains simple.

Since our study focuses on the A&F relay itself, the source-

The authors are with the atlanTTic Research Center, University of Vigo, 36310 Vigo, Spain. (e-mail: {mosquera, valcarce}@gts.uvigo.es). This work was partially funded by the Agencia Estatal de Investigación (Spain) and the European Regional Development Fund (ERDF) through the projects MYRADA (TEC2016-75103-C2-2-R) and WINTER (TEC2016-76409-C2-2-R). Also funded by the Xunta de Galicia (Agrupación Estratéxica Consolidada de Galicia accreditation 2016-2019; Red Temática REdTEIC 2017-2018) and the European Union (European Regional Development Fund - ERDF). Some preliminary results of this paper were presented at IEEE SPAWC 2016 [1].

to-destination link is assumed absent, and the source-to-relay, relay-to-destination, and SI channels are assumed frequency flat, with uniform power allocation over frequency at the source, and non-negligible processing delay at the relay. In our model we consider additive noise at the relay input as well as at the destination, and assume absence of other impairments such as nonlinear distortion due to, e.g., amplifier nonlinearity, receive front-end saturation, or limited dynamic range, which are left for future work. In this way the SI component at the relay input is modelled as a scaled and delayed replica of the signal at the relay output as in [22], [28]–[30], a reasonable assumption whenever SI is sufficiently mitigated at the relay by either passive or active cancellation techniques. Thus, in our model, SI is to be interpreted as residual, and it may be due to estimation errors in the cancellation process. It may also happen that whenever passive means (e.g., antenna placement and radiation pattern optimization) are able to provide sufficient SI mitigation by themselves to avoid saturation of the receive analog front-end [11], [31], the designer may choose not to incorporate active suppression methods in order to keep down relay complexity and cost. This will likely be the case for spectrum sharing networks in which the secondary system acts as a relay for the primary system in exchange for the use of the primary spectrum [32]–[34]. Regardless of its ultimate cause, any residual SI will have to be dealt with by the decoder at the destination node. As will be seen, the PD mode allows to trade off decoding complexity and performance by judicious selection of the spectrum overlap factor.

Our main contributions can be summarized as follows:

1) We introduce the novel PD mode of operation for A&F relays, in which the transmit and receive signals partially overlap in the frequency domain, and which encompasses traditional HD and FD modes as particular cases. The PD relay is shown to be a bandwidth-preserving Linear Periodically Time-Varying (LPTV) system.
2) Exploiting this LPTV property, we numerically evaluate the achievable rate of the PD A&F relay under SI for spectrum overlap factors of the form $\frac{k}{k+1}$ with k integer, by constructing an equivalent (from an information-theoretic point of view) linear time-invariant (LTI) multiple-input multiple-output (MIMO) system.
3) By considering multicarrier modulation with a sufficiently large number of subcarriers, the effect of SI in PD mode is seen to be equivalent to structured inter-carrier interference, allowing an alternative approximation for computing the achievable rate. This results in a much simpler semianalytic expression which is valid for arbitrary values of the spectrum overlap factor, and which shows that with optimal Maximum Likelihood (ML) decoding at destination, the system is ultimately limited by noise, but not by SI.
4) We analyze alternative receiver structures other than the ML decoder, namely direct decoding (treating SI as noise), zero-forcing, minimum mean squared error, and successive interference cancellation, and find semianalytic expressions for their spectral efficiencies.
5) We obtain a closed-form expression for the spectral efficiency of the FD A&F relay under SI with ML decoding at destination and compare it with previous results for direct decoding, showing that treating SI as noise incurs a significant loss.

The paper is organized as follows. After introducing the PD relay operation in Sec. II, its spectral efficiency is analyzed in Secs. III and IV using a time-domain approach and a frequency-domain approximation, respectively. A number of suboptimal receiver architectures with different complexity levels are discussed in Sec. V. In Sec. VI a comparison between HD and FD modes is provided. Numerical results are given in Sec. VII, and conclusions are drawn in Sec. VIII.

Notation: Statistical expectation is denoted by $\mathbb{E}\{\cdot\}$, whereas $\lceil\cdot\rceil$ denotes the ceil function. Lower and uppercase boldface symbols respectively denote vectors and matrices. For a matrix $\mathbf{A}$, its transpose, conjugate transpose, inverse, trace, and determinant are denoted by $\mathbf{A}^T$, $\mathbf{A}^H$, $\mathbf{A}^{-1}$, $\mathrm{tr}\{\mathbf{A}\}$ and $|\mathbf{A}|$, respectively, whereas $[\mathbf{A}]_{i,j}$ denotes its (i,j)-th entry.

II. Partial Duplex Relay

A. System model

Fig. 1 shows the operation of the proposed PD A&F relay. The source transmits a signal $x(t)$, with bandwidth B_u and power $\bar{P}_x$. Upon reaching the relay input, this signal is filtered, frequency-shifted by $f_0 = B - B_u$, and amplified. The input noise $v(t)$ at the relay is Gaussian with power spectral density (psd) M_0 for $0 \leq f \leq B$ and zero otherwise. As long as the passbands of the input and output signals overlap, i.e., $f_0 < B_u$, SI will be present due to coupling from the relay output to its input, with the power gain of the SI path denoted by α. Sufficient input-output isolation is assumed so that SI does not saturate the receive front-end. For low-complexity relay designs, such isolation could be provided by passive techniques alone, whereas with analog/digital active cancellers, our model represents the residual SI due to imperfect cancellation. In the former case the SI power can be expected to be significantly larger than in the latter.

An ideal relay filter frequency response with phase θ_0 and group delay t_0 is assumed, i.e.,

$$L_u(f) = \begin{cases} e^{-j(2\pi f t_0 + \theta_0)}, & 0 \leq f \leq B_u \\ 0, & \text{otherwise.} \end{cases} \tag{1}$$

In practice, the propagation delay of the SI path is much smaller than the group delay t_0 of the relay front-end analog filters, and thus it is neglected. After filtering, the signal is frequency-shifted by multiplication with $e^{j2\pi f_0 t}$, and then amplified with power gain g to yield output power $\bar{P}_y$. The retransmitted signal, denoted by $y(t)$, is corrupted at the destination by additive white Gaussian noise with psd N_0. The source-to-relay and relay-to-destination links are assumed frequency-flat with unity gain, and the direct link from source to destination is assumed absent.

Given the total system bandwidth B, the design parameter is the bandwidth allocated to the input and output signals, $B_u = B - f_0$. This can be expressed in terms of the *overlap factor*

$$\rho \triangleq \frac{B_u}{B} \in \left[\tfrac{1}{2}, 1\right]. \tag{2}$$

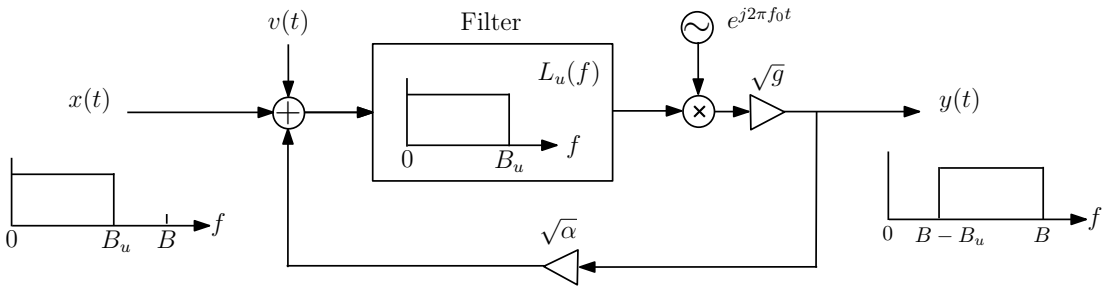

Fig. 1: Baseband-equivalent description of the Partial Duplex A&F relay. In practice, the receive and transmit front-ends incorporate a down-conversion and up-conversion stage, respectively. The difference between the corresponding oscillator frequencies is given by f_0.

The HD mode corresponds to $B_u = B/2$ (i.e., $f_0 = B/2$, or $\rho = \frac{1}{2}$), with non-overlapping input and ouptut spectra; whereas the FD mode is recovered for $B_u = B$ (i.e., $f_0 = 0$, or $\rho = 1$), with complete spectrum overlap. For $\frac{1}{2} < \rho < 1$, the operational mode is termed *Partial Duplex* (PD). The operation of the PD relay can be written in the frequency domain as

$$Y(f) = \sqrt{g} L_u(f-f_0)\left[X(f-f_0) + V(f-f_0) + \sqrt{\alpha} Y(f-f_0)\right] \tag{3}$$

Letting $s(t) \triangleq x(t) + v(t)$, so that $S(f) = X(f) + V(f)$, this recursion can be unfolded to yield

$$Y(f) = \sqrt{g} S(f-f_0) L_u(f-f_0) + \underbrace{\sqrt{g} \sum_{k=1}^{K} (\sqrt{\alpha g})^k S(f-(k+1)f_0) \Pi_{m=1}^{k+1} L_u(f-mf_0)}_{\text{self-interference}} \tag{4}$$

The number of terms K in the SI sum is finite except for $B_u = B$ (FD case), and it is given by

$$K \triangleq \left\lceil \frac{B_u}{B-B_u} \right\rceil - 1 = \left\lceil \frac{\rho}{1-\rho} \right\rceil - 1. \tag{5}$$

This follows from the fact that the filter $L_u(f)$ has bandwidth B_u, whereas the SI undergoes a frequency shift of $f_0 = B - B_u$ each time it loops through the coupling path (see Fig. 1). We assume that the relay uses automatic gain control (AGC), as customary in practical repeaters. The AGC loop automatically adjusts the value of the power gain g to deliver the nominal output power $\bar{P}_y$. Thus, this output power level is independent of the amount of SI at the relay input. In the noiseless SI-free case ($M_0 = 0$, $\alpha = 0$), the relay gain becomes simply $g = \bar{P}_y / \bar{P}_x$.

As performance metric we consider the achievable rate from the source to the final destination through the PD relay, in the absence of a direct link. We define the maximum available signal-to-noise ratios (SNR) at relay and destination, as well as the *loop gain,* respectively as

$$\gamma_{\mathrm{R}} \triangleq \frac{\bar{P}_x}{M_0 B}, \qquad \gamma_{\mathrm{D}} \triangleq \frac{\bar{P}_y}{N_0 B}, \qquad \mathrm{LG} \triangleq \frac{\alpha \bar{P}_y}{\bar{P}_x}. \tag{6}$$

Note that $\frac{1}{\mathrm{LG}}$ can be interpreted as the signal-to-SI ratio at the relay input.

It is illustrative to analyze the power budget of the AGC-equipped relay in the FD case, for which the input-output relation (4) becomes, after letting $f_0 \to 0$ and $K \to \infty$,

$$Y(f) = \frac{\sqrt{g} e^{-j(2\pi f t_0 + \theta_0)}}{1 - \sqrt{\alpha g} e^{-j(2\pi f t_0 + \theta_0)}} S(f) = H(f) S(f), \tag{7}$$

i.e., the FD relay is an infinite impulse response (IIR) LTI system with transfer function $H(f)$. From (4), if we regard the term $\sqrt{g} e^{-j(2\pi f t_0 + \theta_0)} X(f)$ as the useful signal component (with power $g\bar{P}_x$) at the relay output, then the spectrum of the remaining terms (SI) is given by

$$\begin{aligned} Y(f) - \sqrt{g} e^{-j(2\pi f t_0 + \theta_0)} X(f) &= \left[H(f) - \sqrt{g} e^{-j(2\pi f t_0 + \theta_0)} \right] X(f) + H(f) V(f) \\ &= \sqrt{\alpha g} e^{-j(2\pi f t_0 + \theta_0)} H(f) X(f) + H(f) V(f). \end{aligned} \tag{8}$$

Assuming temporarily a noise-free relay ($V(f) = 0$), from (8) the SI power is seen to be $\alpha g \bar{P}_y$. Hence, the signal-to-SI ratio at the relay output is $\frac{g\bar{P}_x}{\alpha g \bar{P}_y} = \frac{1}{\mathrm{LG}}$, i.e., the same as that at its input, so if SI is just regarded as noise, then the performance of the FD relay can be expected to degrade fast as the loop gain increases, leading to overly pessimistic results.

B. PD relay as an LPTV system

For the subsequent analysis, it is important to note that for $B/2 < B_u < B$ (i.e., $\frac{1}{2} < \rho < 1$) the PD relay is not LTI, but rather LPTV. The input-output frequency relationship of a generic LPTV system with input $s(t)$, output $y(t)$ and period T_0 can be written as

$$Y(f) = \sum_{k=-\infty}^{\infty} H_k(f) S\left(f - \frac{k}{T_0}\right) \tag{9}$$

for some transfer functions $\{H_k(f)\}$ [35], [36]. By comparing (9) with (4), and defining

$$L_k(f) \triangleq \prod_{m=1}^{k} L_u(f - mf_0), \quad k = 1, \ldots, K+1, \tag{10}$$

it is clear that the PD relay is LPTV with period $T_0 = 1/f_0$ and

$$H_k(f) = \begin{cases} \sqrt{g} \left(\sqrt{\alpha g}\right)^{k-1} L_k(f), & k = 1, \ldots, K+1, \\ 0, & \text{otherwise.} \end{cases} \tag{11}$$

The support of $H_k(f)$ is within the interval $[B-B_u, B]$, and thus, the PD relay belongs to the particular class of *bandwidth-preserving* LPTV systems, since the size of the spectral region with non-zero frequency content, namely B_u, is the same for both input and output signals. With a non-ideal $L_u(f)$ some out-of-band content will appear, resulting in a spectral efficiency loss.

III. Spectral Efficiency of PD Relay: Time-Domain Approach

Somewhat surprisingly, the information-theoretic analysis of LPTV channels has not been directly addressed until recently. Our derivation follows [37], which was based on the assimilation of the SISO LPTV channel to a multiple-input multiple-output (MIMO) LTI system[1]. The overall system including the source, PD relay, and destination is shown in Fig. 2. The received signal at the destination can be written as

$$r(t) = y(t)+w(t) = \sqrt{g}\int_{-\infty}^{\infty} p(t,\tau)s(t-\tau)d\tau + w(t), \quad (12)$$

which is the time-domain counterpart of (4), with the addition of the noise $w(t)$. An ideal filter with passband $[0, B]$ is assumed at the receiver, so that the psd of the noise $w(t)$ is N_0 for $0 \le f \le B$ and zero otherwise. In terms of the impulse responses $l_k(t) = \int_{-\infty}^{\infty} L_k(f)e^{j2\pi ft}df$, $k = 1, \ldots, K+1$, with $L_k(f)$ given in (10), the response $p(t,\tau)$ is given by

$$p(t,\tau) = \sum_{k=1}^{K+1} \left(\sqrt{g\alpha}\right)^{k-1} l_k(\tau)e^{j2\pi k f_0(t-\tau)}. \quad (13)$$

Note that the input-output relation (12) does correspond to an LPTV system, since $p(t,\tau) = p(t+T_0,\tau)$ with $T_0 = 1/f_0$. In discrete-time form, if the sampling rate is $1/T$, one has

$$\begin{aligned} r(nT) &= \sqrt{g}\sum_{m=-\infty}^{\infty} p(nT,mT)x((n-m)T) \\ &\quad + v'(nT) + w(nT), \quad (14) \\ v'(nT) &= \sqrt{g}\sum_{m=-\infty}^{\infty} p(nT,mT)v((n-m)T), \end{aligned}$$

with the time-varying discrete-time impulse response

$$p(nT,mT) = \sum_{k=1}^{K+1} \left(\sqrt{g\alpha}\right)^{k-1} l_k(mT)e^{j2\pi k f_0 T(n-m)}. \quad (15)$$

Upon choosing $T \le 1/B$, the Nyquist criterion is satisfied for all bandwidths under consideration in Fig. 1. In addition, the sampled system (14) will be LPTV provided that $\frac{T_0}{T}$ is an integer, which will be the period of the LPTV system. These two conditions will simultaneously hold if $\frac{T_0}{T} \in \mathbb{N}$ and $\frac{T_0}{T} \ge \left\lceil \frac{B}{B-B_u} \right\rceil = K+2$. In this section we will assume that $\frac{B}{B-B_u} = q$ is an integer (equivalently, that $\rho = \frac{q-1}{q}$ for some integer q, or $B_u = \left(1-\frac{1}{q}\right)B$), and choose $T = T_0/q = 1/B$. In this way, it can be readily checked that the noise processes $\{v(nT)\}$, $\{w(nT)\}$ will be white with respective variances BM_0, BN_0, which simplifies the analysis. The frequency-domain approximation in Sec. IV will allow to extend the results to $\frac{B}{B-B_u} \notin \mathbb{N}$. Thus, with $f_0T = 1/q$, (15) becomes, for $n = 0, 1, \ldots, q-1$,

$$\begin{aligned} p_n(mT) &\triangleq p(nT, mT) \\ &= \sum_{k=1}^{K+1} (\sqrt{g\alpha})^{k-1} l_k(mT)e^{-j\frac{2\pi}{q}km}e^{j\frac{2\pi}{q}kn}. \quad (16) \end{aligned}$$

Let us define the delay in samples as $\ell \triangleq t_0/T$. For the ideal filter response (1), it can be checked that the term $l_k(mT)e^{-j\frac{2\pi}{q}km}$ in (15) reads as

$$\begin{aligned} l_k(mT)e^{-j\frac{2\pi}{q}km} &= e^{-jk\theta_0}e^{j\pi\left(1-\frac{k}{q}\right)(m-k\ell)} \\ &\quad \times \left(1-\frac{k}{q}\right)\mathrm{sinc}\left[\left(1-\frac{k}{q}\right)(m-k\ell)\right]. \quad (17) \end{aligned}$$

If the delay-bandwidth product of the relay filter is large, i.e., if $Bt_0 = \ell \gg 1$, then (17) is approximately zero outside the interval $0 \le m \le 2k\ell$, and it follows that $p_n(mT) \approx 0$ outside the interval $0 \le m \le \ell_p$, with $\ell_p \triangleq 2(K+1)\ell$, for all $n = 0, 1, \ldots, q-1$.

In the analysis of the PD relay channel, the original scalar model is first transformed into a vector model. Let M be the size of the input signal and noise blocks, defined as

$$\mathbf{x}[n] \triangleq \begin{bmatrix} x(nMT) \\ x((nM+1)T) \\ \vdots \\ x((nM+M-1)T) \end{bmatrix}, \mathbf{v}[n] \triangleq \begin{bmatrix} v(nMT) \\ v((nM+1)T) \\ \vdots \\ v((nM+M-1)T) \end{bmatrix}.$$

Similarly, we define the output block and noise vector respectively as

$$\mathbf{r}[n] \triangleq \begin{bmatrix} r((nM+\ell_p)T) \\ r((nM+\ell_p+1)T) \\ \vdots \\ r((nM+M-1)T) \end{bmatrix}, \mathbf{w}[n] \triangleq \begin{bmatrix} w((nM+\ell_p)T) \\ w((nM+\ell_p+1)T) \\ \vdots \\ w((nM+M-1)T) \end{bmatrix},$$

both having size $M-\ell_p$. Then, the input-output relationship can be expressed in matrix form as

$$\mathbf{r}[n] = \sqrt{g}\mathbf{P}\mathbf{x}[n] + \underbrace{\sqrt{g}\mathbf{P}\mathbf{v}[n] + \mathbf{w}[n]}_{\triangleq \mathbf{z}[n]}, \quad (18)$$

with $\mathbf{z}[n]$ the overall noise vector, and the $(M-\ell_p)\times M$ channel matrix $\mathbf{P}$ given by

$$\mathbf{P} \triangleq \begin{pmatrix} p_{\ell_p}(\ell_pT) & \ldots & p_{\ell_p}(0) & \ldots & 0 \\ \vdots & \ddots & & \ddots & \vdots \\ 0 & \ldots & p_{M-1}(\ell_pT) & \ldots & p_{M-1}(0) \end{pmatrix},$$

where it is implicitly assumed that $p_n(mT)$ is q-periodic in n. The block size M is chosen as an integer multiple of q, so that the input block comprises an integer number of periods. Note that the size of the output block, $M-\ell_p$, is smaller than that of the input block, M. Nevertheless, the impact on spectral efficiency decreases as the block size M grows, and the true capacity $\mathcal{C}$ is obtained as the asymptotic value $\lim_{M\to\infty}\mathcal{C}_M$

[1]This approach traces back to [38], which obtained the capacity of the Gaussian channel with memory by formulating the input-output relationship as a memoryless MIMO channel (although the term "MIMO" was not used at that time).

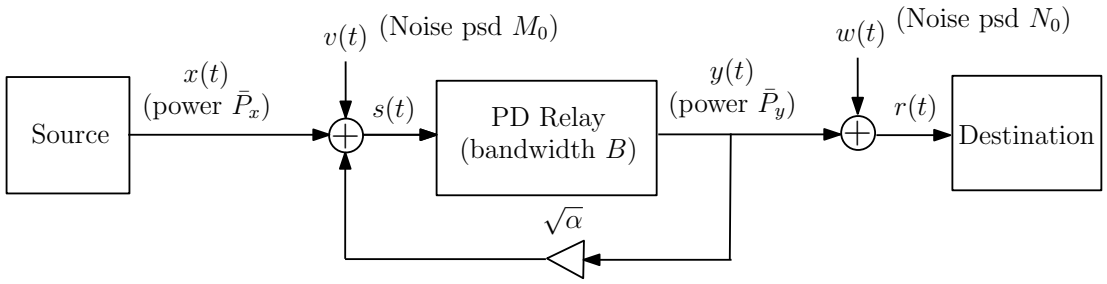

Fig. 2: The source communicates with the destination through a SISO relay with output power $\bar{P}_y$. Part of the retransmitted signal loops back to the relay input, resulting in SI.

[37], with $\mathcal{C}_M$ denoting the achievable rate of the truncated MIMO model with channel matrix $\sqrt{g}\mathbf{P}$, noise covariance matrix $\mathbf{C}_z \triangleq \mathbb{E}\left\{\mathbf{z}[n]\mathbf{z}^H[n]\right\} = BN_0\mathbf{I} + gBM_0\mathbf{P}\mathbf{P}^H$ and input covariance matrix $\mathbf{C}_x \triangleq \mathbb{E}\left\{\mathbf{x}[n]\mathbf{x}^H[n]\right\}$:

$$\mathcal{C}_M = \frac{1}{(M-\ell_p)T}\log_2\left|\mathbf{I} + g\mathbf{C}_z^{-1}\mathbf{P}\mathbf{C}_x\mathbf{P}^H\right| \quad \text{[bps]}. \tag{19}$$

Hence, with $BT = 1$, the corresponding spectral efficiency is

$$\frac{\mathcal{C}}{B} = \lim_{M\to\infty}\frac{1}{M-\ell_p}\log_2\left|\mathbf{I} + g\mathbf{C}_z^{-1}\mathbf{P}\mathbf{C}_x\mathbf{P}^H\right| \quad \text{[bps/Hz]}. \tag{20}$$

Since we are considering frequency-flat channels, the source is assumed to transmit with constant psd in the occupied bandwidth. Then $[\mathbf{C}_x]_{k,l} = C_x((k-l)T)$, with $C_x(\tau) \triangleq \bar{P}_x\ \mathrm{sinc}\left(B_u\tau\right)e^{j2\pi\frac{B_u}{2}\tau}$, which for $B_u = \left(1-\frac{1}{N_{ch}}\right)B$ and $T = \frac{1}{B}$ yields

$$C_x(mT) = \bar{P}_x\ \mathrm{sinc}\left[\left(1-\frac{1}{N_{ch}}\right)m\right]e^{j\pi\left(1-\frac{1}{N_{ch}}\right)m}. \tag{21}$$

To obtain the steady-state value of the relay gain g at which the AGC loop settles, note that the relay output power must equal $\bar{P}_y$, i.e.,

$$g\cdot\frac{\mathrm{tr}\{\mathbf{P}\mathbf{C}_x\mathbf{P}^H\} + BM_0\,\mathrm{tr}\{\mathbf{P}\mathbf{P}^H\}}{M-\ell_p} = \bar{P}_y, \tag{22}$$

which must be solved by numerical means, since $\mathbf{P}$ depends on g. An alternative approach to obtain g will be presented in Sec. IV.

IV. Spectral Efficiency of PD Relay: Frequency-Domain Approach

We present now an alternative approach to computing the capacity of the PD relay, based on the frequency-domain input-output relation (9)-(11), and following standard arguments for frequency-selective LTI channels [39]. The available bandwidth B is sliced into a total of L subcarriers, and the source transmits by using only N of them, with $N < L$, while leaving the remaining $P \triangleq L - N$ subcarriers unused, such that $\frac{N}{L} = \frac{B_u}{B} = \rho$. Thus, the intercarrier spacing is $\Delta f = \frac{B}{L} = \frac{B_u}{N}$, and the frequency offset in Fig. 1 equals $f_0 = B - B_u = P\Delta f$. Transmission is block-based, with blocks of length L to which a cyclic prefix of length ℓ_p is added. The overhead due to the cyclic prefix can be made arbitrarily small as $L\to\infty$.

For LTI channels, this multicarrier approach results in the familiar decoupling of the channel into a set of L independent parallel subchannels with no intercarrier interference (ICI), and with the gain of each subchannel given by the transfer function of the channel at the corresponding frequency bin. However, for the PD relay under SI, ICI will be present due to the fact that the received signal spectrum $Y(f)$ is the superposition of a number of scaled and frequency-shifted replicas $H_k(f)S(f-kf_0)$ of the original spectrum $S(f)$ as seen in (9).

Again, let us assume a sampling rate $T = 1/B$, so that the sampled noise processes $\{v(nT)\}$, $\{w(nT)\}$ are white with powers BM_0 and BN_0, respectively. If we let $\boldsymbol{r}[b]$, $\boldsymbol{x}[b]$, $\boldsymbol{v}[b]$ and $\boldsymbol{w}[b]$ respectively denote the $L\times 1$ vectors given by the Discrete Fourier Transform (DFT) of the bth received signal, transmitted signal, relay noise and destination noise blocks (of length L, or duration LT seconds), then the input-output relation from $\boldsymbol{x}[b]$ to $\boldsymbol{r}[b]$ can be well approximated, for sufficiently large L, as

$$\boldsymbol{r}[b] = \mathbf{H}\boldsymbol{x}[b] + \mathbf{H}\boldsymbol{v}[b] + \boldsymbol{w}[b], \tag{23}$$

where $\mathbf{H}\in\mathbb{C}^{L\times L}$ comprises the ICI coefficients: for $0\le n,m\le L-1$,

$$[\mathbf{H}]_{n,m} = \begin{cases} H_k(n\Delta f), & \text{if } m = n-kP \text{ with } 1\le k\le K+1,\\ 0, & \text{otherwise,}\end{cases} \tag{24}$$

with K as in (5) or, equivalently, $K = \left\lceil\frac{N}{P}\right\rceil - 1$. In the sequel we will omit the block index b for brevity.

In view of (11), $\mathbf{H}$ is seen to be lower triangular; moreover, its first P rows and last P columns are zero. Since the source does not use the last P subcarriers, i.e., the last P entries of $\boldsymbol{x}$ are zero, it follows that $\mathbf{H}\boldsymbol{x}$ can be written as:

$$\mathbf{H}\boldsymbol{x} = \left(\begin{array}{c|c} \mathbf{0}_{P\times N} & \mathbf{0}_{P\times P}\\ \hline \sqrt{g}\mathbf{T}_N\mathbf{D}_N & \mathbf{0}_{N\times P}\end{array}\right)\left(\begin{array}{c}\bar{\boldsymbol{x}}\\ \mathbf{0}_P\end{array}\right) = \left(\begin{array}{c}\mathbf{0}_P\\ \bar{\boldsymbol{y}}\end{array}\right), \tag{25}$$

where $\bar{\boldsymbol{x}}$ and $\bar{\boldsymbol{y}}$ are $N\times 1$, $\mathbf{T}_N\in\mathbb{C}^{N\times N}$ is lower triangular, and $\mathbf{D}_N\in\mathbb{C}^{N\times N}$ is diagonal. Similarly, the first P entries of $\mathbf{H}\boldsymbol{v}$ are all zero. The entries of $\mathbf{D}_N$, $\mathbf{T}_N$ are found from (11) and (24). First, letting $\phi_0 \triangleq 2\pi\Delta f t_0$, one has

$$[\mathbf{D}_N]_{n,n} = e^{-j(n\phi_0+\theta_0)}, \qquad 0\le n\le N-1. \tag{26}$$

Second, the entries $[\mathbf{T}_N]_{n,m}$, $0\le n,m\le N-1$, are zero except when $m = n-kP$ for some $k\in\{0,1,\ldots,K\}$, in which case one has

$$[\mathbf{T}_N]_{n,n-kP} = \left(\sqrt{\alpha g}\right)^k e^{-jk\theta_0}e^{-j\left(nk-P\frac{k(k-1)}{2}\right)\phi_0}. \tag{27}$$

Note in particular that $\mathbf{D}_N\mathbf{D}_N^H = \mathbf{I}_N$, and that $\mathbf{T}_N$ has ones on its diagonal. From (23) and (25) it follows that

$$\bar{\boldsymbol{r}} = \sqrt{g}\mathbf{T}_N\mathbf{D}_N\bar{\boldsymbol{x}} + \sqrt{g}\mathbf{T}_N\mathbf{D}_N\bar{\boldsymbol{v}} + \bar{\boldsymbol{w}}, \tag{28}$$

where $\bar{\boldsymbol{r}}$, $\bar{\boldsymbol{v}}$, $\bar{\boldsymbol{w}}$ comprise the last N entries of $\boldsymbol{r}$, $\boldsymbol{v}$, $\boldsymbol{w}$, respectively. The noise vectors $\bar{\boldsymbol{v}}$ and $\bar{\boldsymbol{w}}$ are zero-mean Gaussian, independent, with respective covariance matrices $BM_0\mathbf{I}_N$ and $BN_0\mathbf{I}_N$, whereas that of $\bar{\boldsymbol{x}}$ is $\frac{L}{N}\bar{P}_x\mathbf{I}_N$ for constant power allocation across $f \in [0, B_u]$ at the source[2]. As a first step, the gain g must be obtained from the PD relay output power:

$$\begin{aligned}\bar{P}_y &= \frac{1}{L}\operatorname{tr}\mathbb{E}\left\{\mathbf{H}(\boldsymbol{x}+\boldsymbol{v})(\boldsymbol{x}+\boldsymbol{v})^H\mathbf{H}^H\right\} \\ &= \frac{g}{L}\operatorname{tr}\mathbb{E}\left\{\mathbf{T}_N\mathbf{D}_N(\bar{\boldsymbol{x}}+\bar{\boldsymbol{v}})(\bar{\boldsymbol{x}}+\bar{\boldsymbol{v}})^H\mathbf{D}_N^H\mathbf{T}_N^H\right\} \\ &= g\left(\frac{\bar{P}_x}{N} + \frac{BM_0}{L}\right)\operatorname{tr}\{\mathbf{T}_N\mathbf{T}_N^H\}. \end{aligned} \tag{29}$$

Hence, $g = \frac{\bar{P}_y}{\bar{P}_x+\rho BM_0}\frac{N}{\operatorname{tr}\{\mathbf{T}_N\mathbf{T}_N^H\}}$. From the expression of $\mathbf{T}_N$, and using $\frac{P}{N} = \frac{1-\rho}{\rho}$, one has

$$\frac{1}{N}\operatorname{tr}\{\mathbf{T}_N\mathbf{T}_N^H\} = \frac{1}{\rho}\sum_{k=0}^{K}(\rho - k(1-\rho))(\alpha g)^k. \tag{30}$$

From (29) and (30), it follows that αg is a solution of the polynomial equation

$$\sum_{k=1}^{K+1}(1-k(1-\rho))(\alpha g)^k = \frac{\rho\,\gamma_{\mathrm{R}}}{\rho+\gamma_{\mathrm{R}}}\mathrm{LG}. \tag{31}$$

The following lemma establishes the uniqueness of the solution; see Appendix A for the proof.

Lemma 1: If $\alpha = 0$ (no SI), then $g = \frac{\bar{P}_y}{\bar{P}_x+\rho BM_0}$. If $\alpha > 0$, then (31) has a single solution satisfying $\alpha g > 0$; in particular, when $\rho = 1$ (FD case), the solution is $\alpha g = \frac{\gamma_{\mathrm{R}}\mathrm{LG}}{1+\gamma_{\mathrm{R}}(1+\mathrm{LG})}$.

Once the relay gain g at which the AGC loop settles has been determined, the sum rate of all carriers can be bounded by the capacity of the channel (28). Since the overall noise vector $\sqrt{g}\mathbf{T}_N\mathbf{D}_N\bar{\boldsymbol{v}}+\bar{\boldsymbol{w}}$ is Gaussian with covariance $BN_0\mathbf{I}_N + gBM_0\mathbf{T}_N\mathbf{T}_N^H$, the following expression is obtained:

$$\frac{\mathcal{C}}{B} = \frac{1}{L}\log_2\left|\mathbf{I}_N + \mu\left(\mathbf{I}_N + \beta\mathbf{T}_N\mathbf{T}_N^H\right)^{-1}\mathbf{T}_N\mathbf{T}_N^H\right|, \tag{32}$$

with γ_{R}, γ_{D} and LG as defined in (6), and having introduced

$$\mu \triangleq g\frac{L}{N}\frac{\bar{P}_x}{BN_0} = \alpha g\frac{\gamma_{\mathrm{D}}}{\rho\mathrm{LG}}, \quad \beta \triangleq g\frac{M_0}{N_0} = \alpha g\frac{\gamma_{\mathrm{D}}}{\gamma_{\mathrm{R}}\mathrm{LG}}. \tag{33}$$

To further develop (32), let us define the matrix $\mathbf{Q}_N$ and its characteristic polynomial as

$$\mathbf{Q}_N \triangleq \left(\mathbf{T}_N\mathbf{T}_N^H\right)^{-1}, \qquad q(\lambda) \triangleq |\mathbf{Q}_N - \lambda\mathbf{I}_N|, \tag{34}$$

allowing to write the determinant in (32) in the following form, to be used in the sequel:

$$\left|\mathbf{I}_N + \mu\left(\mathbf{I}_N + \beta\mathbf{Q}_N^{-1}\right)^{-1}\mathbf{Q}_N^{-1}\right| = \frac{q(-(\mu+\beta))}{q(-\beta)}. \tag{35}$$

To exploit the inherent structure of $\mathbf{Q}_N$, the following lemma will be useful.

[2]This is because the source transmit power is $\bar{P}_x = \frac{1}{L}\operatorname{tr}\mathbb{E}\left\{\boldsymbol{x}\boldsymbol{x}^H\right\}$ and the last $P = L - N$ entries of $\boldsymbol{x}$ are zero.

Lemma 2: The inverse of $\mathbf{T}_N$ is $\mathbf{T}_N^{-1} = \mathbf{I}_N - \sqrt{\alpha g}e^{-j\theta_0}\mathbf{S}_N$, where $\mathbf{S}_N$ is defined entrywise as

$$\begin{aligned}[\mathbf{S}_N]_{n,n-P} &= e^{-jn\phi_0}, \quad n = P, P+1, \ldots, N-1; \\ [\mathbf{S}_N]_{n,m} &= 0, \quad \text{otherwise.}\end{aligned} \tag{36}$$

Lemma 2 is proved by using (27) and (36) to directly verify that $\mathbf{T}_N(\mathbf{I}_N - \sqrt{\alpha g}e^{-j\theta_0}\mathbf{S}_N) = \mathbf{I}_N$. Using this result, one finds that

$$\begin{aligned}\mathbf{Q}_N &= (\mathbf{I}_N - \sqrt{\alpha g}e^{j\theta_0}\mathbf{S}_N^H)(\mathbf{I}_N - \sqrt{\alpha g}e^{-j\theta_0}\mathbf{S}_N) \\ &= \mathbf{I}_N - \sqrt{\alpha g}e^{j\theta_0}\mathbf{S}_N^H - \sqrt{\alpha g}e^{-j\theta_0}\mathbf{S}_N + \alpha g\mathbf{S}_N^H\mathbf{S}_N.\end{aligned}$$

Note now that the matrix $\mathbf{S}_N^H\mathbf{S}_N$ is diagonal, with the first $N-P$ diagonal elements equal to one and the last P equal to zero. Therefore, the entries of $\mathbf{Q}_N$ are zero except along the main diagonal and the P-th super- and sub-diagonals:

$$[\mathbf{Q}_N]_{n,n} = \begin{cases} 1+\alpha g, & 0 \le n \le N-P-1, \\ 1, & N-P \le n \le N-1, \end{cases} \tag{37}$$

$$[\mathbf{Q}_N]_{n,n-P} = -\sqrt{\alpha g}e^{-j(\theta_0+n\phi_0)}, \; P \le n \le N-1, \tag{38}$$

$$[\mathbf{Q}_N]_{n-P,n} = [\mathbf{Q}_N]_{n,n-P}^*, \quad P \le n \le N-1, \tag{39}$$

and $[\mathbf{Q}_N]_{n,m} = 0$ otherwise. The following result holds now; the proof hinges on the structure of $\mathbf{Q}_N$ as exposed by (37)-(39) and can be found in Appendix B.

Theorem 1: Let $q_0(\lambda) = 1$, $q_1(\lambda) = 1-\lambda$ and $q_k(\lambda) = (1+\alpha g-\lambda)q_{k-1}(\lambda) - \alpha g\, q_{k-2}(\lambda)$, $k \ge 2$. Then, with $K = \left\lceil\frac{N}{P}\right\rceil - 1$, the characteristic polynomial $q(\lambda) = |\mathbf{Q}_N - \lambda\mathbf{I}_N|$ is given by

$$q(\lambda) = [q_K(\lambda)]^{(K+1)P-N}\,[q_{K+1}(\lambda)]^{N-KP}. \tag{40}$$

Note in particular that $q(\lambda)$ does not depend on θ_0 or ϕ_0.

Therefore, from (32)-(35), the following expression for the spectral efficiency follows:

$$\begin{aligned}\frac{\mathcal{C}}{B} &= \frac{(K+1)P-N}{L}\log_2\frac{q_K(-(\mu+\beta))}{q_K(-\beta)} \\ &\quad + \frac{N-KP}{L}\log_2\frac{q_{K+1}(-(\mu+\beta))}{q_{K+1}(-\beta)}.\end{aligned} \tag{41}$$

Let $\delta(\rho) \in [0,1)$ be the fractional part of $\frac{\rho}{1-\rho}$, i.e.,

$$\delta(\rho) \triangleq \left\lceil\frac{\rho}{1-\rho}\right\rceil - \frac{\rho}{1-\rho}. \tag{42}$$

Since $K = \left\lceil\frac{\rho}{1-\rho}\right\rceil - 1$, one has $\frac{\rho}{1-\rho} = K + 1 - \delta(\rho)$, so that (41) can be compactly written as

$$\begin{aligned}\frac{\mathcal{C}}{B} &= (1-\rho)\left[\delta(\rho)\log_2\frac{q_K(-(\mu+\beta))}{q_K(-\beta)}\right. \\ &\quad \left. + (1-\delta(\rho))\log_2\frac{q_{K+1}(-(\mu+\beta))}{q_{K+1}(-\beta)}\right].\end{aligned} \tag{43}$$

Thus, given system parameters ρ, LG, γ_{R}, γ_{D}, and once the relay gain is obtained by solving (31), then μ, β are determined via (33), and the spectral efficiency is found by evaluating (43) using the recursive definition of the polynomials $q_k(\lambda)$ in Theorem 1. In addition, closed-form expressions follow from (43) for some particular cases of interest.

- **No SI.** If LG $= 0$, i.e., $\alpha = 0$, then $g = \bar{P}_y/(\bar{P}_x + \rho B M_0)$, $\mu = \frac{\gamma_{\rm R}\gamma_{\rm D}}{\rho(\gamma_{\rm R}+\rho)}$ and $\beta = \frac{\gamma_{\rm D}}{\gamma_{\rm R}+\rho}$. Also, $q_k(\lambda) = (1-\lambda)^k$, $k \geq 0$, so that (43) yields

$$\frac{\mathcal{C}}{B} = \rho \log_2\left(1 + \frac{\gamma_{\rm D}}{\rho} \cdot \frac{\gamma_{\rm R}}{\gamma_{\rm R}+\gamma_{\rm D}+\rho}\right) \quad \text{(no SI)}. \quad (44)$$

- **High SNR at destination.** For $\lambda \ll 0$ one has $q_k(\lambda) \approx (-\lambda)^k$. Hence, as $\gamma_{\rm D} \to \infty$ with $\gamma_{\rm R}$ finite, one has $\mu, \beta \to \infty$, and (43) saturates at $\rho \log_2\left(1 + \frac{\gamma_{\rm R}}{\rho}\right)$ (which is also the limit of (44) as $\gamma_{\rm D} \to \infty$), regardless of LG. Thus, for large SNR at destination, the system is *not limited by SI,* but rather by noise at the relay input.
- **High SNR at relay and destination.** If $\gamma_{\rm R}$ and $\gamma_{\rm D}$ increase at the same rate, so that $\mu \to \infty$ with β constant, then $q_k(-(\mu+\beta)) \approx \mu^k$, and (43) becomes $\frac{\mathcal{C}}{B} \approx \rho \log_2 \gamma_{\rm D} + c_0$, where c_0 depends on (ρ, LG) but not on $(\gamma_{\rm R}, \gamma_{\rm D})$. Thus, SI affects c_0, having the effect of shifting the spectral efficiency vs. $\gamma_{\rm D}$ curve, but it does not affect the pre-log factor, ρ.

V. Receiver Structures

In the general PD relay operation, its time-varying nature results in ICI in the frequency domain as seen in (25) or (28). The decoding of symbols transmitted through channels of the form (28) is a well-studied problem, especially in MIMO systems [39]. As an alternative to the optimal ML receiver, we analyze the performance of four suboptimal detectors: (i) a direct decoding scheme which treats interference as noise, (ii) the zero-forcing (ZF) receiver, (iii) the Linear Minimum Mean Squared Error (LMMSE) receiver, and (iv) the Successive Interference Cancellation (SIC) receiver.

A. Direct decoding

The channel model (28) can be rewritten as

$$\bar{\boldsymbol{r}} = \sqrt{g}\mathbf{D}_N\bar{\boldsymbol{x}} + \sqrt{g}(\mathbf{T}_N - \mathbf{I}_N)\mathbf{D}_N\bar{\boldsymbol{x}} + \sqrt{g}\mathbf{T}_N\mathbf{D}_N\bar{\boldsymbol{v}} + \bar{\boldsymbol{w}}. \quad (45)$$

The first and second terms in the right-hand side of (45) respectively represent the signal part (since $\mathbf{D}_N$ is diagonal) and the ICI (since $(\mathbf{T}_N - \mathbf{I}_N)\mathbf{D}_N$ has zeros on the diagonal). The signal covariance matrix is $\frac{g\bar{P}_x}{\rho}\mathbf{I}_N$, whereas that of the interference plus noise is $\mathbf{C}_{\rm I+N} \triangleq \frac{g\bar{P}_x}{\rho}\widetilde{\mathbf{T}}_N\widetilde{\mathbf{T}}_N^H + gBM_0\mathbf{T}_N\mathbf{T}_N^H + BN_0\mathbf{I}_N$, where $\widetilde{\mathbf{T}}_N \triangleq \mathbf{T}_N - \mathbf{I}_N$. Therefore, the achievable rate of a direct decoding strategy in which subcarriers are independently decoded with the interference term regarded as noise is given by

$$\mathcal{R}_{\rm Dir} = \Delta f \sum_{n=1}^{N} \log_2\left(1 + \rho_n^{\rm Dir}\right), \quad (46)$$

where $\rho_n^{\rm Dir}$ is the signal-to-interference-plus-noise ratio (SINR) at the n-th subcarrier:

$$\rho_n^{\rm Dir} = \frac{g\bar{P}_x/\rho}{[\mathbf{C}_{\rm I+N}]_{n,n}} = \frac{\mu}{1 + \beta\left[\mathbf{T}_N\mathbf{T}_N^H\right]_{n,n} + \mu\left[\widetilde{\mathbf{T}}_N\widetilde{\mathbf{T}}_N^H\right]_{n,n}}, \quad (47)$$

with μ, β as in (33). Since $\widetilde{\mathbf{T}}_N\widetilde{\mathbf{T}}_N^H = \mathbf{T}_N\mathbf{T}_N^H - \mathbf{T}_N - \mathbf{T}_N^H + \mathbf{I}_N$ and $\mathbf{T}_N$ has ones on the diagonal, one has $\left[\widetilde{\mathbf{T}}_N\widetilde{\mathbf{T}}_N^H\right]_{n,n} = \left[\mathbf{T}_N\mathbf{T}_N^H\right]_{n,n} - 1$; and, from (27), the diagonal elements of $\mathbf{T}_N\mathbf{T}_N^H$ can be readily found: writing $n = (k-1)P + m$ with $k \in \{1, \ldots, K+1\}$ and $m \in \{1, \ldots, P\}$,

$$\left[\mathbf{T}_N\mathbf{T}_N^H\right]_{n,n} = \frac{1-(\alpha g)^k}{1-\alpha g}, \quad (48)$$

where αg is obtained from (31). Using (47)-(48), and with $\delta(\rho)$ as in (42), the corresponding spectral efficiency $\frac{\mathcal{R}_{\rm Dir}}{B} = \frac{1}{L}\sum_{n=1}^{N}\log_2\left(1+\rho_n^{\rm Dir}\right)$ can be written as

$$\frac{\mathcal{R}_{\rm Dir}}{B} = (1-\rho)\left[\sum_{k=1}^{K}\log_2\left(1 + \frac{\mu}{1+\beta\frac{1-(\alpha g)^k}{1-\alpha g} + \mu\frac{\alpha g-(\alpha g)^k}{1-\alpha g}}\right) + (1-\delta(\rho))\log_2\left(1 + \frac{\mu}{1+\beta\frac{1-(\alpha g)^{K+1}}{1-\alpha g} + \mu\frac{\alpha g-(\alpha g)^{K+1}}{1-\alpha g}}\right)\right] \quad (49)$$

In the absence of SI ($\alpha = 0$), all log terms in (49) are equal; and since $(1-\rho)(K+1-\delta(\rho)) = \rho$, (49) becomes $\rho\log_2\left(1 + \frac{\gamma_{\rm D}}{\rho}\frac{\gamma_{\rm R}}{\gamma_{\rm R}+\gamma_{\rm D}+\rho}\right)$, i.e., direct decoding is of course optimal, see (44). On the other hand, when $\alpha > 0$ and $\gamma_{\rm D}$, $\gamma_{\rm R}$ go to infinity at the same rate (so that $\mu \to \infty$ whereas β remains bounded), all log terms in (49) tend to finite values except for the one corresponding to $k = 1$ in the summation. Hence, in such regime, (49) behaves as $(1-\rho)\log_2\gamma_{\rm D} + c_{\rm Dir}$ with $c_{\rm Dir}$ independent of $\gamma_{\rm R}$, $\gamma_{\rm D}$, so that the pre-log factor is now $1-\rho$, in contrast with the ML receiver, for which the pre-log factor is ρ as seen in Sec. IV. This shows the detrimental effect of SI when its structure is not exploited in the decoding process. As ρ is increased, SI becomes more pronounced due to the larger overlap of the relay input and output spectra.

B. ZF Receiver

From Lemma 2, the inverse of the channel matrix in (28) is $(\sqrt{g}\mathbf{T}_N\mathbf{D}_N)^{-1} = \frac{1}{\sqrt{g}}\mathbf{D}_N^H(\mathbf{I}_N - \sqrt{\alpha g}e^{-j\theta_0}\mathbf{S}_N)$, which can be implemented with low complexity. After application of this ZF receiver, each subcarrier is independently decoded. The achievable rate with this ZF scheme is $\mathcal{R}_{\rm ZF} = \Delta f\sum_{n=1}^{N}\log_2\left(1+\rho_n^{\rm ZF}\right)$, where $\rho_n^{\rm ZF}$ is the SNR at the n-th subcarrier. Since the covariance matrix of the post-processing noise is $BM_0\mathbf{I}_N + \frac{BN_0}{g}\mathbf{D}_N^H(\mathbf{T}_N^H\mathbf{T}_N)^{-1}\mathbf{D}_N$, one has

$$\rho_n^{\rm ZF} = \frac{\bar{P}_x/\rho}{BM_0 + \frac{BN_0}{g}\left[\mathbf{D}_N^H(\mathbf{T}_N^H\mathbf{T}_N)^{-1}\mathbf{D}_N\right]_{n,n}} = \frac{\mu}{\beta + \left[(\mathbf{T}_N^H\mathbf{T}_N)^{-1}\right]_{n,n}}. \quad (50)$$

From Lemma 2, $(\mathbf{T}_N^H\mathbf{T}_N)^{-1} = \mathbf{I}_N - \sqrt{\alpha g}e^{-j\theta_0}\mathbf{S}_N - \sqrt{\alpha g}e^{j\theta_0}\mathbf{S}_N^H + \alpha g\mathbf{S}_N\mathbf{S}_N^H$. The matrix $\mathbf{S}_N\mathbf{S}_N^H$ is diagonal, with the first $P = L - N$ diagonal elements equal to 0 and the last $N - P$ equal to 1. Hence, $\left[(\mathbf{T}_N^H\mathbf{T}_N)^{-1}\right]_{n,n}$ equals 1 for $n = 1, \ldots, P$ and $1 + \alpha g$ for $n = P+1, \ldots, N$, yielding

$$\frac{\mathcal{R}_{\rm ZF}}{B} = (1-\rho)\log_2\left(1 + \frac{\mu}{1+\beta}\right) + (2\rho - 1)\log_2\left(1 + \frac{\mu}{1+\alpha g+\beta}\right), \quad (51)$$

which behaves as $\rho \log_2 \gamma_{\mathrm{D}} + c_{\mathrm{ZF}}$ when γ_{D}, γ_{R} go to infinity at the same rate. The pre-log factor, ρ, is the same as that of the optimal ML receiver, and in contrast with $1-\rho$ for the direct decoding strategy of Sec. V-A.

C. LMMSE Receiver

Based on the channel model (28), the linear MMSE receiver computes $\hat{\boldsymbol{x}} = \mathbf{F}^H \bar{\boldsymbol{r}}$. The matrix $\mathbf{F}$ is chosen to minimize $\mathbb{E}\left\{\|\bar{\boldsymbol{x}} - \hat{\boldsymbol{x}}\|^2\right\}$, and is found to be

$$\mathbf{F} = \frac{\mu}{\sqrt{g}} \left(\mathbf{I}_N + (\beta+\mu)\mathbf{T}_N \mathbf{T}_N^H\right)^{-1} \mathbf{T}_N \mathbf{D}_N. \tag{52}$$

The achievable rate with the LMMSE receiver is $\mathcal{R}_{\mathrm{LMMSE}} = \Delta f \sum_{n=1}^{N} \log_2\left(1+\rho_n^{\mathrm{LMMSE}}\right)$, with corresponding spectral efficiency

$$\frac{\mathcal{R}_{\mathrm{LMMSE}}}{B} = \frac{\rho}{N} \sum_{n=1}^{N} \log_2\left(1+\rho_n^{\mathrm{LMMSE}}\right), \tag{53}$$

where ρ_n^{LMMSE}, the SINR at the n-th subcarrier, is given by

$$\rho_n^{\mathrm{LMMSE}} = \frac{q_n}{1-q_n},$$

(see e.g. [39]), with q_n the (n,n) entry of the effective channel matrix $\mathbf{F}^H(\sqrt{g}\mathbf{T}_N\mathbf{D}_N)$:

$$\begin{aligned} q_n &= \frac{\mu}{\beta+\mu}\left[\mathbf{T}_N^H\left(\mathbf{T}_N\mathbf{T}_N^H + \frac{1}{\beta+\mu}\mathbf{I}_N\right)^{-1}\mathbf{T}_N\right]_{n,n} \\ &= \frac{\mu}{\beta+\mu}\left(1 - \left[\left(\mathbf{I}_N + (\beta+\mu)\mathbf{T}_N^H\mathbf{T}_N\right)^{-1}\right]_{n,n}\right), \end{aligned}$$

for which it does not seem possible to obtain a closed-form expression. In the high SNR regime ($\mu \to \infty$), the MMSE receiver (52) approaches the ZF receiver $(\sqrt{g}\mathbf{T}_N\mathbf{D}_N)^{-1}$, and therefore the spectral efficiency (53) approaches (51) asymptotically as γ_{D} goes to infinity.

D. Successive Interference Cancellation Receiver

The channel matrix $\sqrt{g}\mathbf{T}_N\mathbf{D}_N$ in (28) is lower triangular, which makes successive decoding attractive. The sequence of symbols in the first carrier $[\bar{\boldsymbol{r}}]_1$ is decoded and used to substract $[\bar{\boldsymbol{x}}]_1$ from the next affected carrier, whose index is $L-N$. The process would continue until all carriers are decoded without interference. This SIC scheme is still suboptimal, because the power of the interference terms is not exploited. Since the diagonal elements of the channel matrix $\sqrt{g}\mathbf{T}_N\mathbf{D}_N$ have all magnitude $\sqrt{g}$, and the covariance matrices of $\bar{\boldsymbol{x}}$ and $\sqrt{g}\mathbf{T}_N\mathbf{D}_N\bar{\boldsymbol{v}} + \bar{\boldsymbol{w}}$ are $\frac{\bar{P}_x}{\rho}\mathbf{I}_N$ and $gBM_0\mathbf{T}_N\mathbf{T}_N^H + BN_0\mathbf{I}_N$ respectively, the achievable rate of the SIC receiver is $\mathcal{R}_{\mathrm{SIC}} = \Delta f \sum_{n=1}^{N} \log_2\left(1+\rho_n^{\mathrm{SIC}}\right)$, with ρ_n^{SIC} the corresponding SINR at the n-th subcarrier:

$$\rho_n^{\mathrm{SIC}} = \frac{g\bar{P}_x/\rho}{BN_0 + gBM_0\left[\mathbf{T}_N\mathbf{T}_N^H\right]_{n,n}} = \frac{\mu}{1+\beta\left[\mathbf{T}_N\mathbf{T}_N^H\right]_{n,n}}. \tag{54}$$

Using (48), the corresponding spectral efficiency is found:

$$\begin{aligned} \frac{\mathcal{R}_{\mathrm{SIC}}}{B} &= (1-\rho)\left[\sum_{k=1}^{K}\log_2\left(1+\frac{\mu}{1+\beta\frac{1-(\alpha g)^k}{1-\alpha g}}\right)\right. \\ &\quad \left. + (1-\delta(\rho))\log_2\left(1+\frac{\mu}{1+\beta\frac{1-(\alpha g)^{K+1}}{1-\alpha g}}\right)\right] \end{aligned} \tag{55}$$

which behaves as $\rho \log_2 \gamma_{\mathrm{D}} + c_{\mathrm{SIC}}$ when γ_{D}, γ_{R} go to infinity at the same rate.

E. Complexity Analysis

The ML decoder achieves the spectral efficiency (43) at the expense of potentially large computational complexity. With $\mathbf{C} = \mathbf{C}^{1/2}\mathbf{C}^{H/2} = BN_0\mathbf{I} + gBM_0\mathbf{T}_N\mathbf{T}_N$ the covariance matrix of the noise term in (28), the ML decoder solves $\min_{\bar{\boldsymbol{x}}\in\mathcal{X}^N} \|\mathbf{C}^{-1/2}\bar{\boldsymbol{r}} - \sqrt{g}\mathbf{C}^{-1/2}\mathbf{T}_N\mathbf{D}_N\bar{\boldsymbol{x}}\|^2$, where $\mathcal{X}$ is the symbol constellation. This requires evaluating the objective function for all possible transmitted vectors $\bar{\boldsymbol{x}}$, hence the computational complexity is exponential in N. With direct decoding, the receiver simply multiplies the received vector $\bar{\boldsymbol{r}}$ in (45) by $\frac{1}{\sqrt{g}}\mathbf{D}_N^H$ to adjust the gain and phase, which takes N complex multiplications (cmults). The ZF decoder compensates the ICI computing $\frac{1}{\sqrt{g}}\mathbf{D}_N^H\mathbf{T}_N^{-1}\bar{\boldsymbol{r}}$; by Lemma 2, the inverse $\mathbf{T}_N^{-1}$ has a sparse structure, allowing implementation of the ZF receiver with $2N-P = N(3-\frac{1}{\rho})$ cmults. On the other hand, the LMMSE receiver multiplies $\bar{\boldsymbol{r}}$ by a matrix with no particular structure, requiring N^2 cmults. Finally, it is readily found that the number of cmults required by the SIC decoder is upper bounded by $\frac{K(K+1)}{2}P$, which in turn is upper bounded by $\frac{N}{2(1-\rho)}$. This goes to infinity as $\rho \to 1$ because the number of interference terms grows accordingly with the spectrum overlap factor. In contrast, the complexity of the ZF receiver remains bounded for all ρ, since $N \le N(3-\frac{1}{\rho}) \le 2N$ for $\rho \in [\frac{1}{2}, 1]$. With these facts in mind, the choice of ρ and the decoding strategy can be determined to trade off complexity and performance, as will be further discussed in Sec. VII.

VI. HD versus FD Operation

High SI levels can be expected to favor HD over FD operation, since the additional bandwidth will not compensate for the degradation due to SI. Motivated by the practical importance of the HD and FD operation modes, we quantify the spectral efficiency in both cases as a function of the SNR and loop gain. The HD spectral efficiency is found by making $\rho = \frac{1}{2}$ in (44):

$$\left.\frac{\mathcal{C}}{B}\right|_{\mathrm{HD}} = \frac{1}{2}\log_2\left(1+\frac{2\gamma_{\mathrm{D}}\gamma_{\mathrm{R}}}{\frac{1}{2}+\gamma_{\mathrm{D}}+\gamma_{\mathrm{R}}}\right). \tag{56}$$

On the other hand, the following result provides the FD spectral efficiency (under ML decoding) in closed form (see Appendix C for the proof). Recall from (7) that the FD relay can be seen as an IIR filter, with closed-loop pole magnitude $\sqrt{\alpha g} = \sqrt{\frac{\gamma_{\mathrm{R}}\mathrm{LG}}{1+\gamma_{\mathrm{R}}(1+\mathrm{LG})}}$ as per Lemma 1. This magnitude approaches 1 as LG increases, so that the complexity of the ML Sequence Estimator (Viterbi algorithm), which increases

$$\left.\frac{\mathcal{C}}{B}\right|_{\mathrm{FD}} = \log_2\left(\frac{1+\gamma_{\mathrm{R}}+\gamma_{\mathrm{D}}+\gamma_{\mathrm{R}}\gamma_{\mathrm{D}}+2\mathrm{LG}\gamma_{\mathrm{R}}+\sqrt{(1+\gamma_{\mathrm{R}}+\gamma_{\mathrm{D}}+\gamma_{\mathrm{R}}\gamma_{\mathrm{D}})^2+4\mathrm{LG}(1+\gamma_{\mathrm{R}})\gamma_{\mathrm{R}}\gamma_{\mathrm{D}}}}{1+\gamma_{\mathrm{R}}+\gamma_{\mathrm{D}}+2\mathrm{LG}\gamma_{\mathrm{R}}+\sqrt{(1+\gamma_{\mathrm{R}}+\gamma_{\mathrm{D}})^2+4\mathrm{LG}\gamma_{\mathrm{R}}\gamma_{\mathrm{D}}}}\right). \quad (57)$$

exponentially with the memory of the channel, may become prohibitive if LG is large.

Lemma 3: As $\rho \to 1$, the spectral efficiency (43) becomes (57), seen at the top of this page.

As the loop gain increases ($\mathrm{LG} \to \infty$), (57) falls to zero, showing the detrimental effect of SI in FD operation. On the other hand, in the absence of SI ($\mathrm{LG} = 0$), (57) reduces to

$$\left.\frac{\mathcal{C}}{B}\right|_{\mathrm{FD}} = \log_2\left(1+\frac{\gamma_{\mathrm{D}}\gamma_{\mathrm{R}}}{1+\gamma_{\mathrm{R}}+\gamma_{\mathrm{D}}}\right) \quad \text{(FD, no SI)}, \quad (58)$$

which agrees with (44) for $\rho = 1$. Note that both (56) and (58) are symmetric in γ_{R}, γ_{D}; thus, performance is limited by $\min\{\gamma_{\mathrm{R}}, \gamma_{\mathrm{D}}\}$. The ratio of (58) to the HD spectral efficiency (56) will tend to 2 only asymptotically as both γ_{R} and γ_{D} go to infinity, but in general it is smaller than 2. A sufficient condition for (58) to be larger than (56) is that $\gamma_{\mathrm{R}}\gamma_{\mathrm{D}} \geq 3$.

High SNR behavior. Consider now the direct decoding strategy (all SI is regarded as noise) applied to the FD case. Using an approach analogous to that in Appendix C, it can be shown that (49) becomes

$$\lim_{\rho\to 1}\frac{\mathcal{R}_{\mathrm{Dir}}}{B} = \log_2\left(1+\frac{\gamma_{\mathrm{D}}\gamma_{\mathrm{R}}}{1+(1+\mathrm{LG})\gamma_{\mathrm{R}}+(1+\mathrm{LG}\,\gamma_{\mathrm{R}})\gamma_{\mathrm{D}}}\right), \quad (59)$$

which is in agreement with the corresponding expression in [28]. Note that, as $\gamma_{\mathrm{D}} \to \infty$, (59) saturates at $\log_2\left(1+\frac{\gamma_{\mathrm{R}}}{1+\mathrm{LG}\gamma_{\mathrm{R}}}\right)$, whereas (57) attains $\log_2(1+\gamma_{\mathrm{R}})$. Thus, with direct decoding, the system is limited by both noise at the relay input *and* SI, whereas with ML decoding the limitation is only due to the noise.

Power control at the relay. An important issue regarding the design of FD relays is that of transmit power optimization [22], [28]. If we regard $\bar{P}_y$ as the maximum available power at the relay and allow for power control, so that the relay transmit power is $P_y = p\,\bar{P}_y$ with $0 \leq p \leq 1$, then the spectral efficiency of the FD relay with direct decoding is given by (59) upon substituting γ_{D} and LG by $p\,\gamma_{\mathrm{D}}$ and $p\,\mathrm{LG}$, respectively. It can be readily checked that the maximum is attained for $p = \min\left\{\sqrt{\frac{1+\gamma_{\mathrm{R}}}{\mathrm{LG}\,\gamma_{\mathrm{R}}\gamma_{\mathrm{D}}}}, 1\right\}$, yielding

$$\lim_{\rho\to 1}\frac{\mathcal{R}_{\mathrm{Dir}}}{B} = \begin{cases} \log_2\left(1+\frac{\gamma_{\mathrm{D}}\gamma_{\mathrm{R}}}{1+(1+\mathrm{LG})\gamma_{\mathrm{R}}+(1+\mathrm{LG}\,\gamma_{\mathrm{R}})\gamma_{\mathrm{D}}}\right), & \mathrm{LG} \leq \frac{1+\gamma_{\mathrm{R}}}{\gamma_{\mathrm{R}}\gamma_{\mathrm{D}}}, \\ \log_2\left(1+\frac{\gamma_{\mathrm{D}}\gamma_{\mathrm{R}}}{\mathrm{LG}\,\gamma_{\mathrm{R}}+\gamma_{\mathrm{D}}+2\sqrt{\mathrm{LG}\,(1+\gamma_{\mathrm{R}})\gamma_{\mathrm{R}}\gamma_{\mathrm{D}}}}\right), & \mathrm{LG} \geq \frac{1+\gamma_{\mathrm{R}}}{\gamma_{\mathrm{R}}\gamma_{\mathrm{D}}}. \end{cases} \quad (60)$$

Therefore, having the FD relay transmit at full power is not necessarily optimal when SI is regarded as noise, as observed in [18], [22], [28]: if SI levels are sufficiently large, as determined by the condition $\mathrm{LG} \geq \frac{1+\gamma_{\mathrm{R}}}{\gamma_{\mathrm{R}}\gamma_{\mathrm{D}}}$, then it is better to reduce the transmit power. On the other hand, the expression resulting from replacing γ_{D} and LG by $p\,\gamma_{\mathrm{D}}$ and $p\,\mathrm{LG}$, respectively, in (57) turns out to be monotonically increasing in $p \in [0, 1]$; therefore, with ML decoding, having the relay transmit at full power is optimal.

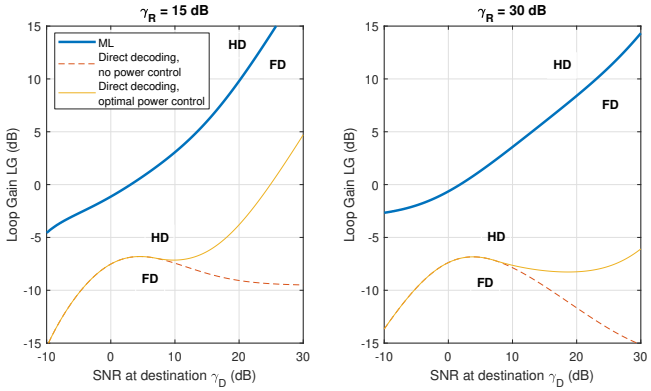

Fig. 3: HD vs. FD performance. For the ML and direct decoding strategies, the corresponding lines represent the boundary of regions in which one of these modes outperforms the other.

HD vs. FD. The regions for which one operational mode (HD or FD) outperforms the other are depicted in Fig. 3, where the lines correspond to the boundary (set of points such that the spectral efficiencies of the FD and HD modes become equal) for ML and direct decoding (with and without power control for the latter). With ML decoding, and for any LG value, FD outperforms HD if γ_{D} is sufficiently large. On the other hand, with direct decoding and full-power transmission, FD cannot perform better than HD as soon as $\mathrm{LG} > -7$ dB, regardless of the SNR. Power control improves the situation, but the distance with respect to ML decoding remains significant.

VII. Results

The spectral efficiency of the PD A&F relay network with uniform power allocation across the input bandwidth B_u, and for different receiver strategies, is illustrated in Figs. 4 and 5. The operation point is determined by the bandwidth ratio $\rho = B_u/B \in \left[\frac{1}{2}, 1\right]$, the SNR at the relay ($\gamma_{\mathrm{R}}$) and destination ($\gamma_{\mathrm{D}}$), and the magnitude of the coupling (loop gain LG), see (6). The different curves in Figs. 4 and 5 are labeled as follows:

- *No SI:* this upper bound corresponds to the SI-free case ($\mathrm{LG} = 0$), and is given by (44).
- *ML:* spectral efficiency of an optimum ML decoder, given by (43), from the frequency-domain approach of Sec. IV.
- *SIC:* spectral efficiency with a SIC receiver, given by (55).
- *LMMSE:* spectral efficiency with a linear MMSE-based receiver, computing as in Sec. V-C. Since a closed-form expression is lacking, a total of $N = 1000$ subcarriers was used in the numerical computations.
- *ZF:* spectral efficiency with a ZF-based linear receiver, given by (51).
- *Direct Dec.:* spectral efficiency with a direct decoding strategy, given by (49).

- *TD:* These points are computed following the time-domain approach of Sec. III, for $\rho = \frac{N_{ch}-1}{N_{ch}}$, $N_{ch} = 2, \ldots, 10$. A truncated sinc was assumed for the filter $L_u(f)$, with $Bt_0 = 5N_{ch}$. The block size M was taken as $M = \left(\left\lceil \frac{\ell_p+1}{N_{ch}} \right\rceil + \kappa \right) N_{ch}$, with $\kappa = 300$.
- *Full Duplex:* spectral efficiency of the Full-Duplex relay, given by the closed-form expression in (57).

Each of Figs. 4 and 5 shows results for three values of γ_{D} (5, 10 and 20 dB) and two SI environments: $\mathrm{LG} = -5$ dB (weak coupling, i.e., SI power below signal power) and $\mathrm{LG} = 5$ dB (strong coupling, i.e., SI power above signal power). In Fig. 4 the SNR at the relay is $\gamma_{\mathrm{R}} = 30$ dB, corresponding to a scenario with a high quality source-to-relay link resulting from careful relay deployment. On the other hand, in Fig. 5 a low value $\gamma_{\mathrm{R}} = 10$ dB is considered.

A close match is observed between the spectral efficiency values of the optimal ML decoder obtained via the time-domain approach of Sec. III and those obtained under the frequency-domain approximation of Sec. IV. Note that the latter approach does not rely on the existence of a periodic behavior of the PD relay and is computationally much simpler; additionally, it applies to any value of $\rho \in [\frac{1}{2}, 1]$. The jagged appearance of the curves with the bandwidth ratio ρ in strong coupling scenarios is due to our assumptions of ideal brickwall filter responses and rectangular power spectral densities, which make the analysis tractable. As a result, the number of SI terms K in (5) increases by one as ρ crosses the values of the form $\frac{2}{3}$, $\frac{3}{4}$, $\frac{4}{5}$,..., producing abrupt changes in the derivative of the spectral efficiency at those points.

For a given $(\gamma_{\mathrm{R}}, \gamma_{\mathrm{D}})$ pair, and as soon as $\rho > \frac{1}{2}$, the performance of the PD relay significantly degrades under SI regardless of the receiver strategy, as can be seen by comparing the left and right columns in each of Figs. 4 and 5. This degradation, which is more pronounced for lower SNR values, is particularly severe for the direct decoding approach; this fact brings out the need to take SI into account at the receiver even in weak coupling scenarios.

With high SNR at the relay (Fig. 4), SIC detection outperforms LMMSE and ZF strategies, with close-to-optimal performance except in situations with strong coupling and low SNR at destination, for which the gap to optimality becomes wider. When the SNR at the relay is low (Fig. 5), LMMSE or even ZF decoding provide a more competitive alternative to SIC detection, especially for high SNR at destination: the SIC scheme seems to be particularly sensitive to noise at the relay input. It is also observed that LMMSE generally outperforms ZF, and that they perform similarly under high SNR conditions, as expected.

As mentioned in Sec. IV, with ML decoding the performance of the PD relay is not limited by SI, in the sense that the effect of SI can be overcome if the SNR at destination γ_{D} is sufficiently large. In Figs. 4 and 5 it is observed that, under strong coupling, the advantage of PD ($\rho > \frac{1}{2}$) with respect to HD ($\rho = \frac{1}{2}$) is in general small (if any), unless γ_{D} is significantly large (20 dB). On the other hand, in weak coupling scenarios, spectral efficiency monotonically improves with the bandwidth ratio ρ, and the gain already becomes significant for moderate values of γ_{D}. This improvement is obtained at the cost of the additional complexity required at the receiver to manage the SI, because the number K of SI terms to handle increases with ρ, up to $K = \infty$ for $\rho = 1$ (FD mode). In this way, selection of an intermediate PD mode with $\frac{1}{2} < \rho < 1$ allows to trade off performance (in terms of spectral efficiency) and decoding complexity. As an example, in the setting of Fig. 4 with $\gamma_{\mathrm{R}} = 30$ dB, $\gamma_{\mathrm{D}} = 20$ dB and $\mathrm{LG} = -5$ dB, the PD modes corresponding to $\rho = \frac{2}{3}$ (for which $K = 1$), $\rho = \frac{3}{4}$ ($K = 2$) and $\rho = \frac{4}{5}$ ($K = 3$) provide improvements in spectral efficiency of up to 22%, 33% and 40% with respect to the HD mode, respectively, and these gains are achievable with SIC decoding. This is further illustrated in Fig. 6, which shows the variation of the spectral efficiencies of the HD, FD and PD ($\rho = \frac{3}{4}$) modes with the SNR at destination γ_{D}, in a scenario with $\gamma_{\mathrm{R}} = 20$ dB: as soon as γ_{D} is sufficiently large, a sizable improvement in spectral efficiency is achievable with this PD mode over HD, at a small fraction of the computational cost of FD; the stronger the coupling, the larger the required value of γ_{D} to achieve such gain. Alternatively, the PD relay is more robust to SI for larger values of γ_{D}: this can be seen in Fig. 7, which shows the variation of the spectral efficiencies with the loop gain. For $\gamma_{\mathrm{D}} = 10$ dB, the efficiency of the PD and FD modes fall below that of HD for loop gain values above 3 dB, whereas for $\gamma_{\mathrm{D}} = 20$ dB, the crossing point shifts to $\mathrm{LG} = 9$ dB. Thus, although in low SNR scenarios HD may be the preferred option, there is clear incentive to contemplate using a PD mode when the source-to-relay and relay-to-destination links are of sufficiently good quality. By choosing an appropriate value of ρ, an appropriate tradeoff between receiver complexity and spectral efficiency can be achieved.

VIII. Conclusions

Generalizing the well-known Half-Duplex and Full-Duplex cases, an Amplify-and-Forward relay with partial overlap between input and output spectra has been proposed and analyzed in the presence of SI at the relay. Its spectral efficiency for different overlap ratios has been obtained by exploiting the bandwidth-preserving LPTV nature of this Partial Duplex relay. The time- and frequency-domain approaches considered are equivalent from an information-theoretic point of view, and thus they yield matching results, although the former only applies to particular values of the overlap factor. In addition, the frequency-domain approach suggests alternative decoding schemes and allows to obtain a number of closed-form expressions which are useful in the analysis. An important conclusion is that proper management of SI (which should not be simply regarded as noise) becomes mandatory in order to reap the benefits of spectrum overlap; in fact, with optimal decoding, the relay system is ultimately limited by noise, but not by SI. With this in mind, several suboptimal decoding strategies at the receiver were also analyzed, among which Succesive Interference Cancellation emerges as a promising technique, performing close to the optimal ML decoder in high SNR. By effectively limiting the number of in-band SI terms, the proposed Partial Duplex mode provides a means

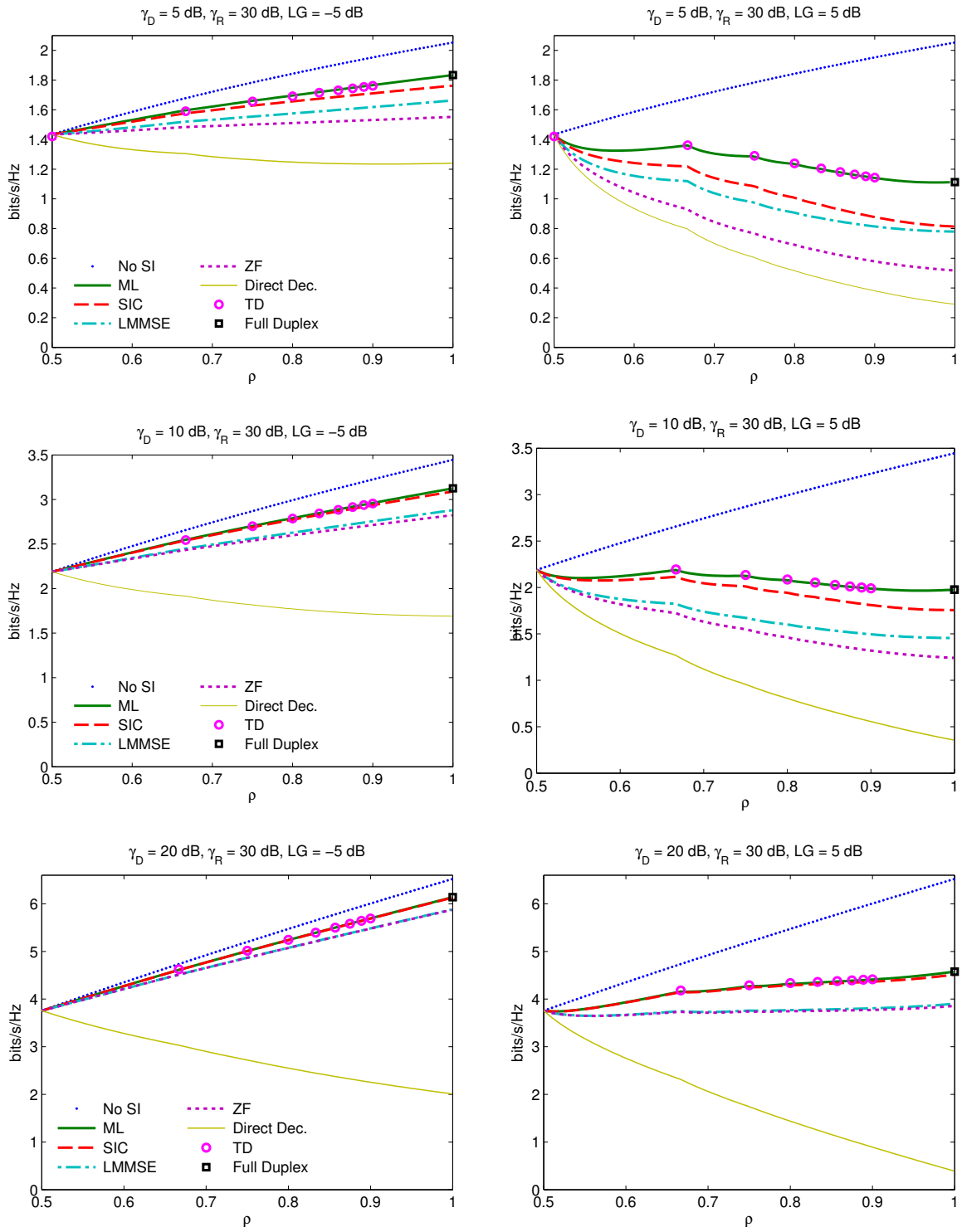

Fig. 4: Spectral efficiency of the A&F PD relay vs. $\rho = B_u/B$ for a good source-to-relay link ($\gamma_{\mathrm{R}} = 30$ dB). Left: weak coupling ($\mathrm{LG} = -5$ dB); right: strong coupling ($\mathrm{LG} = 5$ dB); $\gamma_{\mathrm{D}} = 5$ dB (top), 10 dB (middle) and 20 dB (bottom).

to trade off spectral efficiency and receiver complexity. These results find application in relaying scenarios where complete SI cancellation is either impossible, because of estimation errors, or undesirable, in order to reduce relay complexity.

Appendix A
Proof of Lemma 1

If $\alpha = 0$, then from (30), $\frac{1}{N}\,\mathrm{tr}\{\mathbf{T}_N\mathbf{T}_N^H\} = 1$, and substituting this in (29) yields $g = \frac{\bar{P}_y}{\bar{P}_x + \rho B M_0}$.

Assume now $\alpha > 0$. If $\rho = 1$, then $K = +\infty$ and (31)

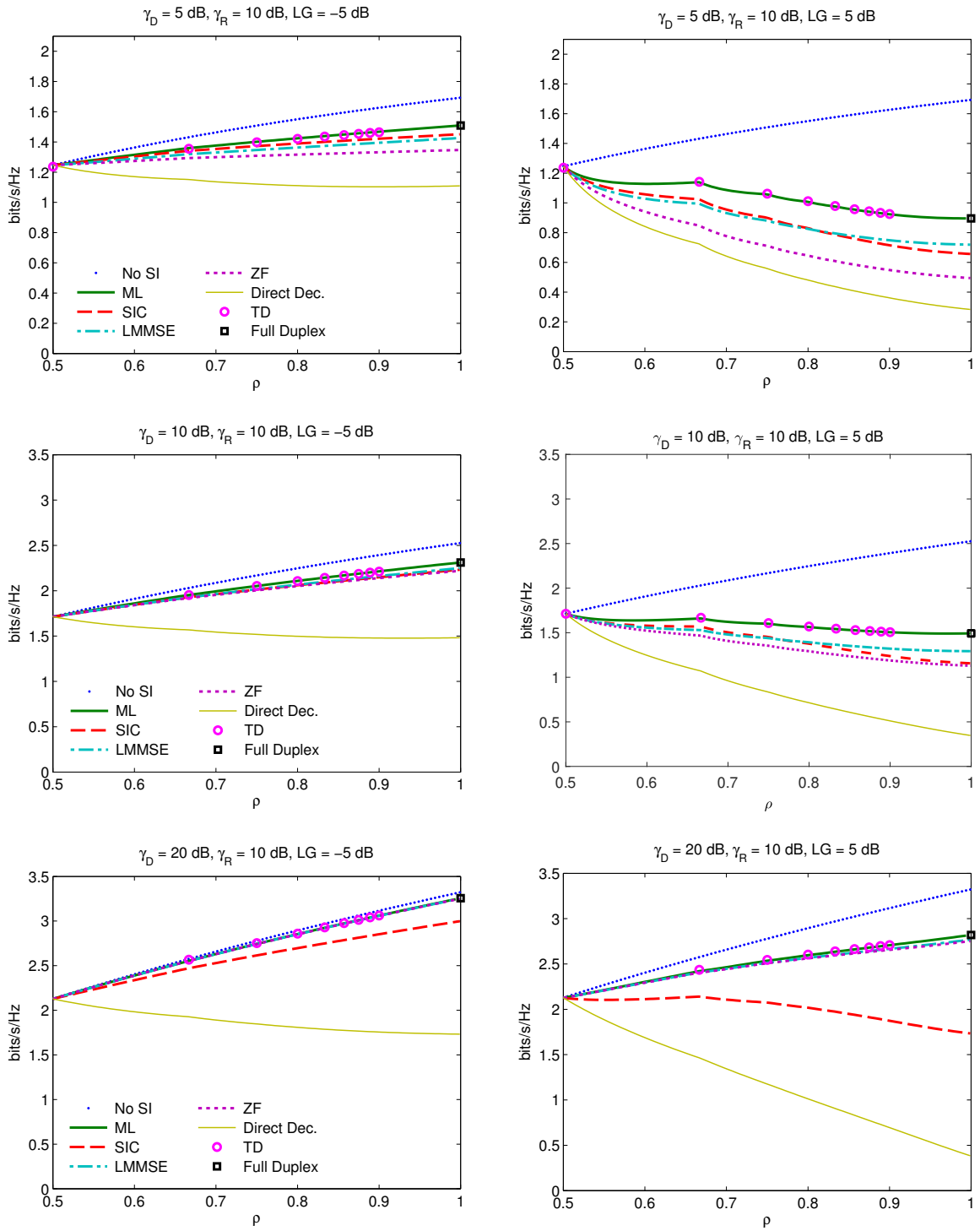

Fig. 5: Spectral efficiency of the A&F PD relay vs. $\rho = B_u/B$ for a poor source-to-relay link ($\gamma_{\rm R} = 10$ dB). Left: weak coupling (LG $= -5$ dB); right: strong coupling (LG $= 5$ dB); $\gamma_{\rm D} = 5$ dB (top), 10 dB (middle) and 20 dB (bottom).

reads as $\sum_{k=1}^{\infty}(\alpha g)^k = \frac{\rho\gamma_{\rm R}}{\rho+\gamma_{\rm R}}{\rm LG}$. This implies $0 \le \alpha g < 1$ (note that αg is the squared magnitude of the pole of the FD relay transfer function, which therefore is stable), and $\frac{\alpha g}{1-\alpha g} = \frac{\rho\gamma_{\rm R}}{\rho+\gamma_{\rm R}}{\rm LG}$, from which $\alpha g = \frac{\gamma_{\rm R}{\rm LG}}{1+\gamma_{\rm R}(1+{\rm LG})}$.

If $\rho < 1$, consider the polynomial $p(s) = -c + \sum_{k=1}^{K+1}(1 - k(1-\rho))s^k$, with $c \triangleq \frac{\rho\gamma_{\rm R}}{\rho+\gamma_{\rm R}}{\rm LG} \ge 0$. First, note that the coefficients $1 - k(1-\rho)$ are positive: for $k = 1, \ldots, K+1$,

$$1-k(1-\rho) \ge 1-(K+1)(1-\rho) = 1-\left\lceil \frac{\rho}{1-\rho} \right\rceil (1-\rho). \quad (61)$$

Write now $K+1 = \left\lceil \frac{\rho}{1-\rho} \right\rceil = \frac{\rho}{1-\rho} + \delta$, with $\delta \in [0, 1)$. Then

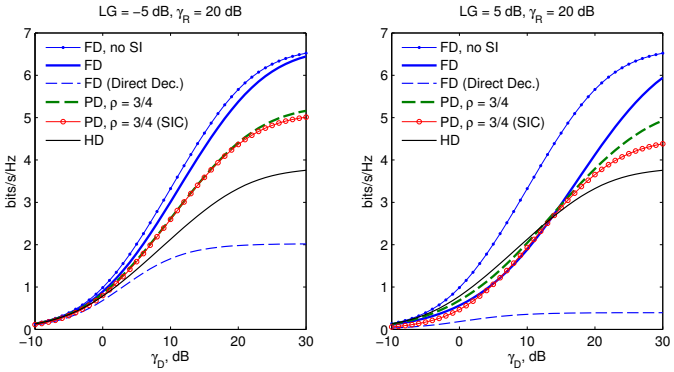

Fig. 6: Spectral efficiencies of the FD, PD ($\rho = \frac{3}{4}$) and HD relay modes vs. SNR at destination. ML decoding is assumed, except where indicated.

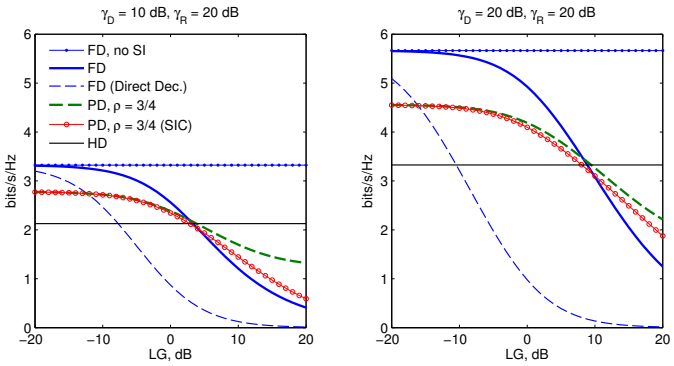

Fig. 7: Spectral efficiencies of the FD, PD ($\rho = \frac{3}{4}$) and HD relay modes vs. loop gain. ML decoding is assumed, except where indicated.

(61) reads

$$1-k(1-\rho) \geq 1-(\rho+\delta(1-\rho)) = (1-\rho)(1-\delta) > 0, \quad (62)$$

since $\rho < 1$. From the positivity of these terms it follows that $\lim_{s\to\infty} p(s) = +\infty$. Since $p(0) = -c \leq 0$, $p(s)$ has at least a root in $s \in [0, +\infty)$. Moreover, $p'(s) = \sum_{k=1}^{K+1}(1-k(1-\rho))ks^{k-1} \geq 0$ for all $s \geq 0$, so that $p(s)$ is monotonically increasing in $s \in [0, +\infty)$. Hence, the root is unique.

Appendix B
Proof of Theorem 1

Given $P \in \mathbb{N}$, $a, b, \phi \in \mathbb{R}$ and $c \in \mathbb{C}$, let us define the matrices $\mathbf{A}_M(a, c, \phi) \in \mathbb{C}^{M\times M}$ and $\mathbf{C}_M(c, \phi) \in \mathbb{C}^{M\times P}$ as follows: for $M > P$, $\mathbf{A}_M(a, c, \phi)$ is given by (63) at the top of next page, whereas

$$\mathbf{C}_M(c,\phi) = \left(\begin{array}{c} \mathbf{0}_{(M-P)\times P} \\ \hline ce^{j(M-P)\phi} \\ \\ \ddots \\ \\ ce^{jM\phi} \end{array}\right). \quad (64)$$

For $M \leq P$, $\mathbf{A}_M(a, c, \phi) = a\mathbf{I}_M$ and

$$\mathbf{C}_M(c,\phi) = \left(\begin{array}{c|c} \mathbf{0}_{M\times(P-M)} & \begin{array}{c} ce^{j\phi} \\ \\ \ddots \\ \\ ce^{jM\phi} \end{array} \end{array}\right). \quad (65)$$

For $N > P$, define $\mathbf{Z}_N(a, b, c, \phi) \in \mathbb{C}^{N\times N}$ as

$$\mathbf{Z}_N(a,b,c,\phi) = \left(\begin{array}{cc} \mathbf{A}_{N-P}(a,c,\phi) & \mathbf{C}_{N-P}(c,\phi) \\ \mathbf{C}^H_{N-P}(c,\phi) & b\mathbf{I}_P \end{array}\right). \quad (66)$$

Note that the matrix $\mathbf{Q}_N - \lambda\mathbf{I}_N$, with $\mathbf{Q}_N$ defined by (37)-(39), can be written as $\mathbf{Q}_N - \lambda\mathbf{I}_N = \mathbf{Z}_N(a, b, c, \phi)$ with $a = 1+\alpha g-\lambda$, $b = 1-\lambda$, $c = -\sqrt{\alpha g}e^{j\theta_0}$ and $\phi = \phi_0$. To compute $|\mathbf{Z}_N(a, b, c, \phi)|$, we use the expression for the determinant of partitioned matrices to obtain

$$|\mathbf{Z}_N(a,b,c,\phi)| = b^P \left|\mathbf{A}_{N-P}(a,c,\phi) - \frac{1}{b}\mathbf{C}_{N-P}(c,\phi)\mathbf{C}^H_{N-P}(c,\phi)\right|. \quad (67)$$

If $P < N \leq 2P$, (67) readily evaluates to

$$|\mathbf{Z}_N(a,b,c,\phi)| = b^P\left(a - \frac{|c|^2}{b}\right)^{N-P}, \qquad P < N \leq 2P. \quad (68)$$

On the other hand, for $N > 2P$, since

$$\mathbf{C}_{N-P}(c,\phi)\mathbf{C}^H_{N-P}(c,\phi) = \left(\begin{array}{cc} \mathbf{0} & \\ & |c|^2\mathbf{I}_P \end{array}\right), \quad (69)$$

it follows that

$$\begin{aligned}\mathbf{A}_{N-P}(a,c,\phi) - \frac{1}{b}\mathbf{C}_{N-P}(c,\phi)\mathbf{C}^H_{N-P}(c,\phi) \\ = \mathbf{Z}_{N-P}\left(a, a-\frac{|c|^2}{b}, c, \phi\right),\end{aligned} \quad (70)$$

so that the following recursion is obtained for $N > 2P$:

$$|\mathbf{Z}_N(a,b,c,\phi)| = b^P\left|\mathbf{Z}_{N-P}\left(a, a-\frac{|c|^2}{b}, c, \phi\right)\right|. \quad (71)$$

Let us define the scalar sequence

$$\tilde{\eta}_1(a,b,c) = b, \qquad \tilde{\eta}_n(a,b,c) = a - \frac{|c|^2}{\tilde{\eta}_{n-1}(a,b,c)}, \quad n \geq 2. \quad (72)$$

From (68) and (71), one finds that, with $K = \lceil \frac{N}{P} \rceil - 1$,

$$|\mathbf{Z}_N(a,b,c,\phi)| = \tilde{\eta}^{N-KP}_{K+1}(a,b,c)\prod_{n=1}^{K}\tilde{\eta}^P_n(a,b,c), \quad (73)$$

which is independent of ϕ and $\angle c$. Alternatively, letting $\eta_k(a, b, c) \triangleq \prod_{n=1}^{k}\tilde{\eta}_n(a, b, c)$, one has

$$|\mathbf{Z}_N(a,b,c,\phi)| = [\eta_K(a,b,c)]^{(K+1)P-N}[\eta_{K+1}(a,b,c)]^{N-KP}, \quad (74)$$

where $\eta_k(a, b, c)$ is obtained recursively as follows: $\eta_1(a, b, c) = b$, $\eta_2(a, b, c) = ab - |c|^2$ and, for $k > 2$,

$$\begin{aligned}\eta_k &= \eta_{k-1}\tilde{\eta}_k = \eta_{k-1}\left(a - \frac{|c|^2}{\tilde{\eta}_{k-1}}\right) \\ &= \eta_{k-1}\left(a - \frac{|c|^2\eta_{k-2}}{\eta_{k-1}}\right) = a\eta_{k-1} - |c|^2\eta_{k-2}.\end{aligned}$$

Particularizing this recursion for $a = 1 + \alpha g - \lambda$, $b = 1 - \lambda$, $|c|^2 = \alpha g$, Theorem 1 is proved.

$$\mathbf{A}_M(a,c,\phi)=\begin{pmatrix} a & \mathbf{0}_{P-1}^T & ce^{j\phi} & & & & \\ \mathbf{0}_{P-1} & \ddots & \mathbf{0}_{P-1} & \ddots & & & \\ c^*e^{-j\phi} & \mathbf{0}_{P-1}^T & a & & \ddots & & \\ & \ddots & & \ddots & & ce^{j(M-P)\phi} & \\ & & \ddots & & \ddots & \mathbf{0}_{P-1} & \\ & & & c^*e^{-j(M-P)\phi} & \mathbf{0}_{P-1}^T & a & \end{pmatrix} \tag{63}$$

APPENDIX C
PROOF OF LEMMA 3

In order to compute the asymptotic value of (43) as $\rho \to 1$, we take $\rho = \frac{N}{N+1}$ and let $N \to \infty$. With this, one has $K+1 = N$ and $\delta(\rho) = 0$, so that, from (43), $\frac{C}{B} = \frac{1}{K+2}\log_2 \frac{q_{K+1}(-(\mu+\beta))}{q_{K+1}(-\beta)}$. Clearly, as $K \to \infty$, $\frac{q_{K+1}(-(\mu+\beta))}{q_{K+1}(-\beta)}$ must diverge, or otherwise $\frac{C}{B}$ would go to zero. In fact, for $\frac{C}{B}$ to have a finite, positive limit as $K \to \infty$, one must have $\frac{q_{K+1}(-(\mu+\beta))}{q_{K+1}(-\beta)} \approx ab^K$ asymptotically, for some finite $a > 0$, $b > 1$, and then the spectral efficiency becomes

$$\begin{aligned} &\lim_{K\to\infty} \frac{1}{K+2}\frac{q_{K+1}(-(\mu+\beta))}{q_{K+1}(-\beta)} \\ &= \lim_{K\to\infty}\left(\frac{\log_2 a}{K+2} + \frac{K+1}{K+2}\log_2 b\right) = \log_2 b. \end{aligned}$$

Note that, upon defining $r_k(\lambda) \triangleq \frac{q_k(-\lambda)}{q_{k-1}(-\lambda)}$, one has $b = \lim_{k\to\infty}\frac{r_k(\mu+\beta)}{r_k(\beta)}$. From the recursive definition of $q_k(\lambda)$ in Theorem 1, one has $r_1(\lambda) = 1+\lambda$ and

$$r_k(\lambda) = 1 + \alpha g + \lambda - \frac{\alpha g}{r_{k-1}(\lambda)}, \qquad k \geq 2. \tag{75}$$

Since $\alpha g \geq 0$, it is readily shown by induction that $r_k(\lambda) \geq 1+\lambda$ for all $\lambda \geq 0$.

Let $h = \lim_{k\to\infty}\alpha g$ and $r(\lambda) = \lim_{k\to\infty} r_k(\lambda)$. Then, taking the limit as $k \to \infty$ in both sides of (75), one finds that $r^2(\lambda) - (1+h+\lambda)r(\lambda) + h = 0$. One of the solutions to this quadratic equation can be shown to be no larger than 1, whereas the other is given by

$$r(\lambda) = \frac{1}{2}\left[1 + h + \lambda + \sqrt{(1+h+\lambda)^2 - 4h}\right]. \tag{76}$$

Now, from Lemma 1, one has $h = \frac{\mathrm{LG}\,\gamma_{\mathrm{R}}}{1+(1+\mathrm{LG})\gamma_{\mathrm{R}}}$ for $\rho \to 1$. Using this and (33), it follows that $\mu \to \mu_1 \triangleq \frac{\gamma_{\mathrm{R}}\gamma_{\mathrm{D}}}{1+(1+\mathrm{LG})\gamma_{\mathrm{R}}}$ and $\beta \to \beta_1 \triangleq \frac{\gamma_{\mathrm{D}}}{1+(1+\mathrm{LG})\gamma_{\mathrm{R}}}$ as $\rho \to 1$. Hence,

$$b = \lim_{k\to\infty}\frac{r_k(\mu+\beta)}{r_k(\beta)} = \frac{r(\mu_1+\beta_1)}{r(\beta_1)}, \tag{77}$$

from which (57) follows by straightforward manipulation.

REFERENCES

[1] C. Mosquera and R. López-Valcarce, "Bandwidth allocation in partial duplex relaying," in *IEEE Int. Workshop Signal Process. Adv. Wireless Commun.*, Jul. 2016.

[2] J. N. Laneman, D. N. C. Tse, and G. W. Wornell, "Cooperative diversity in wireless networks: Efficient protocols and outage behavior," *IEEE Trans. Inf. Theory*, vol. 50, no. 12, pp. 3062–3080, Dec. 2004.

[3] D. Soldani and S. Dixit, "Wireless relays for broadband access," *IEEE Commun. Mag.*, vol. 46, no. 3, pp. 58–66, Mar. 2008.

[4] S. Berger, M. Kuhn, A. Wittneben, T. Unger, and A. Klein, "Recent advances in amplify-and-forward two-hop relaying," *IEEE Commun. Mag.*, vol. 47, no. 7, pp. 50–56, Jul. 2009.

[5] L. Jimenez Rodriguez, N. Tran, and T. Le-Ngoc, *Amplify-and-Forward Relaying in Wireless Communications*. Springer, 2015.

[6] A. Sabharwal, P. Schniter, D. Guo, D. W. Bliss, S. Rangarajan, and R. Wichman, "In-band full-duplex wireless: Challenges and opportunities," *IEEE J. Sel. Areas Commun.*, vol. 32, no. 9, pp. 1637–1652, Sep. 2014.

[7] G. Liu, F. R. Yu, H. Ji, V. C. M. Leung, and X. Li, "In-band full-duplex relaying: A survey, research issues, and challenges," *IEEE Commun. Surveys Tuts.*, vol. 17, no. 2, pp. 500–524, 2015.

[8] Z. Zhang, K. Long, A. V. Vasilakos, and L. Hanzo, "Full-duplex wireless communications: Challenges, solutions, and future research directions," *Proc. IEEE*, vol. 104, no. 7, pp. 1369–1409, Jul. 2016.

[9] L. Song, R. Wichman, Y. Li, and Z. Han, *Full-Duplex Communications and Networks*. Cambridge University Press, 2017.

[10] T. Riihonen, S. Werner, and R. Wichman, "Mitigation of loopback self-interference in full-duplex MIMO relays," *IEEE Trans. Signal Process.*, vol. 10, no. 59, pp. 5983–5993, Dec. 2011.

[11] M. Duarte, C. Dick, and A. Sabharwal, "Experiment-driven characterization of full-duplex wireless systems," *IEEE Trans. Wireless Commun.*, vol. 11, no. 12, pp. 4296–4307, Dec. 2012.

[12] D. Bharadia, E. McMilin, and S. Katti, "Full duplex radios," in *Proc. ACM SIGCOMM Conf.*, 2013, pp. 375–386.

[13] M. Heino, D. Korpi, T. Huusari, E. Antonio-Rodriguez, S. Venkatasubramanian, T. Riihonen, L. Anttila, K. Haneda, R. Wichman, and M. Valkama, "Recent advances in antenna design and interference cancellation algorithms for in-band full-duplex relays," *IEEE Commun. Mag.*, vol. 53, no. 5, pp. 91–101, May 2015.

[14] K. Shibuya, "Broadcast-wave relay technology for digital terrestrial television broadcasting,," *Proc. IEEE*, vol. 94, no. 1, pp. 269–273, Jan. 2006.

[15] J. Y. Choi, M.-S. Hur, Y.-W. Suh, J.-S. Baek, Y.-T. Lee, and J.-S. Seo, "Interference cancellation techniques for digital on-channel repeaters in T-DMB system," *IEEE Trans. Broadcast.*, vol. 57, no. 1, pp. 46–56, Jan. 2011.

[16] R. Lopez-Valcarce, E. Antonio-Rodriguez, C. Mosquera, and F. Perez-Gonzalez, "An adaptive feedback canceller for full-duplex relays based on spectrum shaping," *IEEE J. Sel. Areas Commun.*, vol. 30, no. 8, pp. 1566–1577, Sep. 2012.

[17] N. Shende, O. Gurbuz, and E. Erkip, "Half-duplex or full-duplex relaying: A capacity analysis under self-interference," in *Proc. 47th Annual Conf. Inf. Sci. Syst.*, 2013, pp. 207–211.

[18] L. Jimenez Rodriguez, N. H. Tran, and T. Le-Ngoc, "Optimal power allocation and capacity of full-duplex AF relaying under residual self-interference," *IEEE Wireless Commun. Lett.*, vol. 3, no. 2, pp. 233–236, Apr. 2014.

[19] ——, "Performance of full-duplex AF relaying in the presence of residual self-interference," *IEEE J. Sel. Areas Commun.*, vol. 32, no. 9, pp. 1752–1764, Sep. 2014.

[20] N. Zlatanov, E. Sippel, V. Jamali, and R. Schober, "Capacity of the Gaussian two-hop full-duplex relay channel with residual self-interference," *IEEE Trans. Commun.*, vol. 65, no. 3, pp. 1005–1021, Mar. 2017.

[21] Z. Chen, T. Q. S. Quek, and Y.-C. Liang, "Spectral efficiency and relay energy efficiency of full-duplex relay channel," *IEEE Trans. Wireless Commun.*, vol. 16, no. 5, pp. 3162–3175, May 2017.

[22] T. Riihonen, S. Werner, and R. Wichman, "Hybrid full-duplex/half-duplex relaying with transmit power adaptation," *IEEE Trans. Wireless Commun.*, vol. 10, no. 9, pp. 3074–3085, Sep. 2011.

[23] ——, "Spatial loop interference suppression in full-duplex MIMO relays," in *Proc. 43rd Ann. Asilomar Conf. Signals, Syst. Comput.*, 2009, pp. 1508–1512.

[24] Y. Y. Kang and J. H. Cho, "Capacity of MIMO wireless channel with full-duplex amplify-and-forward relay," in *IEEE Int. Symp. Personal, Indoor Mobile Radio Commun.*, 2009, pp. 117–121.

[25] T. M. Kim and A. Paulraj, "Outage probability of amplify-and-forward cooperation with full duplex relay," in *IEEE Wireless Commun. Netw. Conf.*, 2012, pp. 75–79.

[26] X. Li, C. Tepeledenlioglu, and H. Senol, "Channel estimation for residual self-interference in full duplex amplify-and-forward two-way relays," *IEEE Trans. Wireless Commun.*, vol. 16, no. 8, pp. 4970–4983, Aug. 2017.

[27] K. Yamamoto, K. Haneda, H. Murata, and S. Yoshida, "Optimal transmission scheduling for a hybrid of full- and half-duplex relaying," *IEEE Commun. Lett.*, vol. 15, no. 3, pp. 305–307, Mar. 2011.

[28] T. Riihonen, S. Werner, and R. Wichman, "Comparison of full-duplex and half-duplex modes with a fixed amplify-and-forward relay," in *IEEE Wireless Commun. Netw. Conf.*, 2009, pp. 207–211.

[29] D. Moya Osorio, E. E. Benitez Olivo, H. Alves, J. C. S. Santos Filho, and M. Latva-aho, "Exploiting the direct link in full-duplex amplify-and-forward relaying networks," *IEEE Signal Process. Lett.*, vol. 22, no. 10, pp. 1766–1770, May 2015.

[30] K. Muranov, B. Smida, and N. Devroye, "On channel equalization for full-duplex relay networks," in *IEEE Int. Conf. Commun.*, May 2017.

[31] E. Everett, A. Sahai, and A. Sabharwal, "Passive self-interference suppression for full-duplex infrastructure nodes," *IEEE Trans. Wireless Commun.*, vol. 13, no. 2, pp. 680–694, Feb. 2014.

[32] Y. Pei and Y.-C. Liang, "Resource allocation for device-to-device communications overlaying two-way cellular networks," *IEEE Trans. Wireless Commun.*, vol. 12, no. 7, pp. 3611–3621, Jul. 2013.

[33] G. Zhang, K. Yang, P. Liu, and J. Wei, "Power allocation for full-duplex relaying-based D2D communication underlaying cellular networks," *IEEE Trans. Veh. Technol.*, vol. 64, no. 10, pp. 4911–4916, Oct. 2015.

[34] A. Zappone, B. Matthiesen, and E. A. Jorswieck, "Energy efficiency in MIMO underlay and overlay device-to-device communications and cognitive radio systems," *IEEE Trans. Signal Process.*, vol. 65, no. 4, pp. 1026–1041, Feb. 2017.

[35] P. Vanassche, G. Gielen, and W. Sansen, "Symbolic modeling of periodically time-varying systems using harmonic transfer matrices," *IEEE Trans. Comput.-Aided Design Integr. Circuits Syst.*, vol. 21, no. 9, pp. 1011–1024, Sep. 2002.

[36] C. Mosquera, S. Scalise, and G. Taricco, "Spectral characterization of feedback linear periodically time-varying systems," in *IEEE Int. Conf. Acoust., Speech, Signal Process.*, vol. 2, 2002, pp. 1209–1212.

[37] N. Shlezinger and R. Dabora, "On the capacity of narrowband PLC channels," *IEEE Trans. Commun.*, vol. 63, no. 4, pp. 1191–1201, Apr. 2015.

[38] L. Brandenburg and A. Wyner, "Capacity of the Gaussian channel with memory: The multivariate case," *Bell System Technol. J.*, vol. 53, no. 5, pp. 745–778, May 1974.

[39] D. Tse and P. Viswanath, *Fundamentals of Wireless Communication*. Cambridge University Press, 2005.